Analytical modelling of the effect of morphological fluctuations on the transverse elastic behaviour of unidirectional fibre reinforced composites

Jennifer Blondel, Sébastien Joannès, Eveline Hervé-Luanco

Analytical modelling of the effect of morphological fluctuations on the transverse elastic behaviour of unidirectional fibre reinforced composites

J. Blondel[a,c], S. Joannès[a,*], E. Hervé-Luanco[b,a,*]

[a] *MINES ParisTech, PSL University, Centre des Matériaux (CMAT), CNRS UMR 7633, BP 87 91003 Evry Cedex, France*
[b] *Université de Versailles, Saint-Quentin en Yvelines, 45 Avenue des Etats-Unis, F-78035 Versailles Cedex, France*
[c] *Manufacture Française des Pneumatiques Michelin, 23 Place des Carmes Déchaux, 63040 Clermont Ferrand Cedex 9, France*

Abstract

This paper proposes to take into account the influence of some morphological fluctuations – often observed in unidirectional composite materials – on the modelling of the elastic behaviour of such materials. This work relies on a Generalized Self-Consistent Scheme coupled with a Morphologically Representative Pattern based approach. An analytical model is proposed to deal with "non-percolated" or trapped matrix regions. Closed-form analytical expressions are provided to investigate different kinds of morphological fluctuation effects on the effective transverse elastic behaviour. Finally some examples are given to illustrate the effectiveness of this approach.

Keywords: Homogenization, Fibre reinforced composites, Micromechanical models, Morphologically Representative Patterns, Generalized Self-Consistent Scheme, Fluctuations of morphology

*Corresponding authors
Email addresses: sebastien.joannes@mines-paristech.fr (S. Joannès),

List of Acronyms & Symbols

Acronyms

EHM	Equivalent Homogeneous Medium 15
FEM	Finite Element Method 8
GHW	Refers to the results published in Gusev et al. (2000) 30
GSCS	Generalized Self-Consistent Scheme 10
MRP	Morphologically Representative Pattern 10
RVE	Representative Volume Element 11
UD	Unidirectional (fibre-reinforced composites) 7
ZC	Refers to the results published in Zimmer and Cost (1970) 30

Subscripts, superscripts and brackets

$\bullet$	Represents an arbitrary (0, 1, 2)-tensor field or a matrix variable
$\underline{\bullet}$	Defines a first-order tensor (vector)
$\underset{\sim}{\bullet}$	Defines a second-order tensor
$\underset{\approx}{\bullet}$	Defines a fourth-order tensor
$\bullet^{(i_\lambda)}$ or $\bullet_{i_\lambda}$	Phase index inside the pattern λ, $i_\lambda \in \{1, \ldots, n_\lambda\}$

eveline.herve@uvsq.fr (E. Hervé-Luanco)

$\bullet^{(k)}$ or $\bullet_k$	The letter k is used generically to designate any phase (k). It can be the phase index $\bullet^{(i)}$ or $\bullet_i$, $i \in \{1, 2, \ldots, n+1\}$ or the phase index inside the pattern λ, $i_\lambda \in \{1, \ldots, n_\lambda\}$
$\bullet^{[j]}$	An estimate of $\bullet$ during the iteration process
$\bullet^{\mathrm{f}}$, $\bullet^{\mathrm{m}}$ or $\bullet^{\mathrm{eff}}$	Related to "fibre", "matrix" or "effective" properties
$\bullet^{\textcircled{\lambda}}$ or $\bullet_{\textcircled{\lambda}}$	Indicates the pattern dependency
$\bullet^{\boxed{\lambda}}$ or $\bullet_{\boxed{\lambda}}$	Identity transformation defined for two patterns and two phases, $\boxed{\lambda} \equiv \mathrm{Id}\,(\lambda)$ with $\boxed{1} = 1$ and $\boxed{2} = 2$
$\bullet^{\blacksquare\boldsymbol{\lambda}}$ or $\bullet_{\blacksquare\boldsymbol{\lambda}}$	Complementary transformation defined for two patterns and two phases, $\blacksquare\boldsymbol{\lambda} \equiv \mathrm{Cp}\,(\lambda)$ with $\blacksquare\mathbf{1} = 2$ and $\blacksquare\mathbf{2} = 1$
$\langle\bullet\rangle_{\Omega_\square}$	Average volume fraction of any $\bullet$ expression over the domain $\Omega_\square$
$\{\underset{\subseteq\bullet}{\mathsf{A}_p}\}$	When $\bullet$ needs to be expanded, $\bullet$ can be, partially or completely, split into several parts: $\{\underset{\subseteq\bullet}{\mathsf{A}_1}\}$, $\{\underset{\subseteq\bullet}{\mathsf{A}_2}\}$, …; $\{\underset{\subseteq\bullet}{\mathsf{A}_p}\}$, $p \in \mathbb{N}$, represents all these parts. When $\bullet$ can be written in different forms, $\{\underset{\subseteq\bullet}{\mathsf{B}_p}\}$, $\{\underset{\subseteq\bullet}{\mathsf{C}_p}\}$, … are used. When only one part is needed, index is omitted

Material constants and parameters

μ_{23}	Shear modulus
ν	Poison's ratio
E	Young's modulus

54	k_{23}	Transverse bulk modulus
55	$\underset{\approx}{C}$	Elastic stiffness tensor

56 **Other Symbols**

57	$\underline{x}$	Position vector, i.e. $\underline{x} = x_1\underline{e_1} + x_2\underline{e_2} + x_3\underline{e_3}$ or $\underline{x} = r\underline{e_r} + x_1\underline{e_1}$
58	$\left(\underline{e_1}, \underline{e_2}, \underline{e_3}\right)$	Cartesian orthonormal basis set
59	$\left(\underline{e_r}, \underline{e_\theta}, \underline{e_1}\right)$	Cylindrical orthonormal basis set
60	(x_1, x_2, x_3)	Cartesian coordinates of $\underline{x}$ in the basis $\left(\underline{e_1}, \underline{e_2}, \underline{e_3}\right)$
61	(r, θ, x_1)	Cylindrical coordinates of $\underline{x}$ in the basis $\left(\underline{e_r}, \underline{e_\theta}, \underline{e_1}\right)$
62	Ω	Domain of material whose effective properties are sought
63	Ω_λ	Domain of the pattern λ, partition of Ω
64	Ω_i	Domain of phase (i), partition of Ω
65	Ω_{i_λ}	Domain of phase (i) inside the pattern λ, partition of Ω_i
66	n	Number of phases
67	N_λ	Number of "Morphological Representative Pattern" families
68	n_λ	Number of phases inside pattern λ
69	f	Volume fraction of phase (1), in the case $N_\lambda = 2$ and $n_\lambda = 2$
70		for each pattern; i.e. $f = f_1$
71	f_i	Volume fraction of phase (i)

m_λ	Volume fraction of pattern λ
m	Volume fraction of the "direct" pattern, in the case $N_\lambda = 2$ and $n_\lambda = 2$ for each pattern; i.e. $m = m_1$
c_{i_λ}	Volume fraction of phase (i) inside pattern λ
$c_{i\textcircled{\lambda}}$	Volume fraction of the "ith" phase inside pattern λ
c	Volume fraction of phase (1) inside the "direct" pattern, in the case $N_\lambda = 2$ and $n_\lambda = 2$ for each pattern; i.e. $c = c_{1_1} = c_{1\textcircled{1}}$
R_i	Outer radius of phase (i) lying within the radii R_{i-1} and R_i
$\underline{T}$	Stress vector
$\underline{T}^0$	Applied stress vector
T_i	Stress vector component along $\underline{e_i}$
$\underline{u}$	Displacement vector
$\underline{u}^0$	Displacement vector applied to each pattern, homogeneous conditions
$\underline{u}^{\mathrm{g}}$	"Given" displacement vector applied to the equivalent homogeneous configuration, homogeneous conditions
u_i	Displacement vector component along $\underline{e_i}$
$\underline{\underline{\sigma}}$	Stress tensor
$\underline{\underline{\varepsilon}}$	Strain tensor

$\underset{\sim}{\varepsilon}^0$	Strain tensor such that $\underline{u}^0 = \underset{\sim}{\varepsilon}^0.\underline{x}$ is applied to each pattern
$\underset{\sim}{E}$	Strain tensor such that $\underline{u}^{\mathrm{g}} = \underset{\sim}{E}.\underline{x}$ is applied to the equivalent homogeneous configuration
$\mathcal{A}_{i_\lambda}$	Average intensity concentration for phase (i_λ)
$\underset{\approx}{\mathcal{A}}_i$	Average intensity concentration tensor for phase (i)
Bold	Bold notation for rectangular arrays i.e. rectangular arrays such as $\mathbf{V}$, $\boldsymbol{J}$, $\boldsymbol{N}$ or $\boldsymbol{Q}$ with components denoted Q_{kl} for example
$\boldsymbol{Q}$ or $\boldsymbol{Q}^*$	Transfer matrices
A_k, B_k, C_k and D_k	Integration constants for each phase (k) in the case of an in-plane transverse shear mode
A_{i_λ} and D_{i_λ}	Constants for phase (i_λ)

1. Introduction

1.1. Evaluating the transverse elastic properties of unidirectional composites

Knowing and anticipating how a structure will deform when subjected to a load is a daily challenge for engineers. Depending on their anisotropy, composite materials can exhibit a strong dependence on the direction in which loads are applied. It is clear that a single unidirectional (UD) ply, for example reinforcing the rubber of a tire, will exhibit a considerable resistance to deformation if the load is applied along the direction of the reinforcement. In contrast, this same ply will undergo a large deformation if the load is now applied in a non-longitudinal direction. To design efficient composite structures and take advantage of the anisotropy, engineers need to characterize or predict the load-deformation material response for all the directions in which loads may occur. Regarding transverse properties, experimental characterization is always a tedious procedure and result uncertainties are often large. These complications provide a strong practical motivation for the development of models which can be used to predict the material performance.

However, this does not mean that models remove the underlying difficulties. If the prediction of UD longitudinal properties is rarely complicated, transverse properties are more affected by interactions between the constituents and predicting accurately the transverse properties is always challenging. Models taking into account the morphological distribution of the phases, in addition to their volume fractions, are required to obtain realistic predictions for the transverse properties of such UD composite materials.

Morphological variabilities and fibre packing strongly influence the transverse linear elastic behaviour of these composites. Numerous and varied methods have already been proposed in order to predict effective properties of such a multi-phases medium. Existing solutions include, on the one hand, full-field approaches – as the Finite Element Method (FEM) for example – requiring to model the microstructure in details. Such methods require complex[1] mesh operations, especially when the fibres get very close or when functionally graded materials are considered. On the other hand, mean-field approaches are based on a single inclusion problem and unlike full-field approaches, only statistical information about the microstructure is needed. Both approaches have their advantages and this work is focused on an efficient, fast and cost-effective analytical mean-field model to take into account morphological fluctuations at the microscopic scale, in order to predict the transverse linear elastic shear and bulk moduli of unidirectional composites.

1.2. A rational microstructure model

As explained previously, this work is devoted to the study of the elastic behaviour of fibre-reinforced composites with different distributions of fibres. Restricting the attention to cylindrical shape and transverse isotropic elasticity, we can refer to Hashin and Rosen's (1964) composite assemblage or to Christensen and Lo's (1979) three-phase model which deal with two-phases coaxial cylinder for a two-phases material. A model has

[1]The two-dimensional models dealt with in the present investigation are nevertheless far more simple than the three-dimensional ones require in the case of macroscopically isotropic particulate composites, such as in Bardella et al. (2018).

been developed in Hervé and Zaoui (1995) to predict the elastic behaviour of heterogeneous fibre-reinforced composites including the case of coated fibre-reinforced composites, usually referred to as the $(n+1)$-phase model[2]. This work has also provided the elastic strain and stress fields in an infinite medium constituted of an n-layered transversely isotropic cylindrical inclusion, surrounded by a transversely isotropic cylindrical matrix subjected to uniform conditions at infinity. These fields have been given in a simpler form in Hervé-Luanco (2020). From that, we can study the transverse elastic behaviour of more complex morphologies regarding the way the fibres are distributed inside the matrix and by also accounting for fibres that can have a functionally graded behaviour. These concerns lead directly, on the one hand, to more than one pattern[3], and, on the other hand to more than two phases in each pattern.

The way used here to take into account complex morphologies is to add as many elementary patterns as needed like in Marcadon et al. (2007) or in Majewski et al. (2017) in the case of particle-reinforced composites having size effects, or in Diani and Gilormini (2014) in the case of linear viscoelasticity of nano-reinforced polymers with an interphase, or in Bilger et al. (2007), Bardella and Genna (2001) and Bardella et al. (2018) in the case of porous materials. This latter case, dealing with macroscopically isotropic particulate composites, is particularly relevant to show that

[2]It should be noted that the three-phase model proposed in Christensen and Lo (1979) corresponds also to the $(n+1)$-phase model developed in Hervé and Zaoui (1995) in the particular case of $n = 2$.

[3]A "pattern" contains a "representative disposition of some of the constitutive mechanical phases", as defined by Bornert et al. (1996).

the present study makes sense. Although the materials are very different, in Bardella et al.'s paper (2018) it is shown that the method adopted in the present investigation, using representative patterns to account for complex morphologies, works very well even with an extremely large filler volume fraction.

If a biphasic matrix-inclusion material is considered, at low volume fraction of inclusions, there is no doubt that the matrix is a continuous and percolating phase as opposed to inclusions which are distributed discontinuously. If the volume fraction of inclusions increases sufficiently a network of percolating aggregates can be formed. The matrix is then trapped by aggregates which makes it lose its continuity and leads to a "phase inversion" phenomenon as discussed in Albérola et al.'s paper (1994). In this specific case of two patterns with two phases in each pattern, using an "inverse" pattern – where the inclusion surrounds the matrix – allows to model this phenomenon (Albérola et al., 1994; Mélé et al., 2005).

In this work, the Generalized Self-Consistent Scheme (GSCS) used in Hervé and Zaoui (1995) and in Hervé-Luanco (2020) is coupled with the Morphologically Representative Pattern (MRP) based approach developed by Bornert et al. (1996) in order to take into account local morphological fluctuations and heterogeneous distribution of fibres. Analytical estimates are provided for both effective transverse shear and bulk moduli. In this paper, the approach followed by Marcadon et al. (2007) for particle-reinforced composites in the case of two patterns with two phases has been generalized in the case of: 1) fibre-reinforced composites 2) for any number of patterns with any number of phases inside each pattern like in Hervé-Luanco and Joannès (2016a). In this latter paper a model has been developed to predict

the transverse properties of a fibre-reinforced composite in the case of transport phenomena. In a second article (Joannès and Hervé-Luanco, 2016b), the authors have used their model to study the influence of fibre packing effects on the transverse properties of the composites regarding transport phenomena.

In the present paper, a MRP-based approach is coupled to the $(n+1)$-phase model thanks to a rearrangement of the transfer matrices in terms of their dependence on the behaviour of a given phase as shown in Hervé-Luanco (2020). It is organized as follows: Section 2 is devoted to the development of the model. Closed-form equations are given for the transverse shear and bulk moduli. In section 3, the model is applied in the case of two patterns with two phases inside each pattern. An example of application is given to highlight the possibilities of the presented model. Two comparisons with experimental data are presented in section 4.

2. Extension of the $(n+1)$-phase model by using a MRP-based approach

2.1. Introduction

Let us consider the configuration defined in Hervé and Zaoui (1995) where the elementary pattern representing the microstructure is a n-phase cylindrical inclusion which is embedded in an infinite matrix subjected to homogeneous boundary conditions at infinity (Figure 1). Each phase is homogeneous, linearly elastic and transversely isotropic with the axis of transverse isotropy along the direction of the fibre.

Let us assume first that the Representative Volume Element (RVE) of the studied microstructure is a Hashin assemblage of cylindrical domains

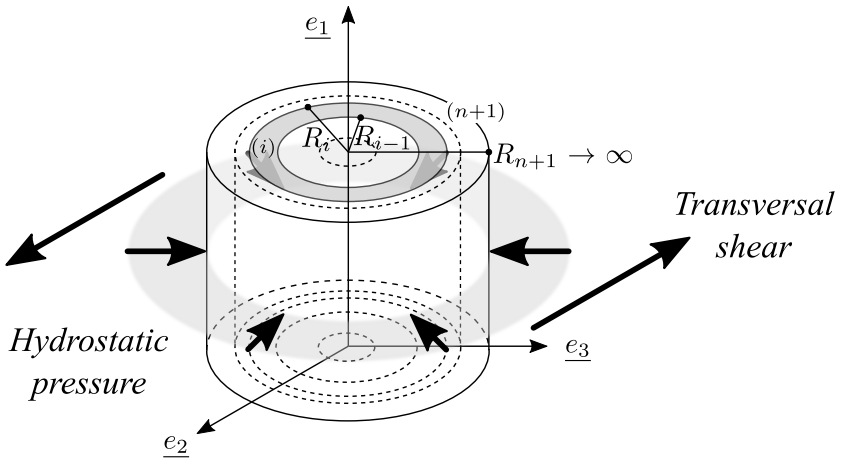

Figure 1: One single elementary pattern made of a n-layered cylindrical inclusion embedded in an infinite matrix, i.e. phase $(n+1)$.

consisting of a set of N_λ families (see Figure 2) of homothetic identical finite composite domains whose material content is known. These families are called here "pattern", they are made of different phases and this microstructure can be referred to as a generalized Hashin's assemblage of patterns. The configuration under study is referred to a Cartesian rectangular coordinate system in the basis $\left(\underline{e_1}, \underline{e_2}, \underline{e_3}\right)$ thus allowing to locate any point from the origin O by its position vector $\underline{x} = x_1\underline{e_1} + x_2\underline{e_2} + x_3\underline{e_3}$. Direction given by $\underline{e_1}$ is parallel to the fibre longitudinal axis while $\left(O, \underline{e_2}, \underline{e_3}\right)$ define the transverse plane. A cylindrical coordinates system with the same origin and the orthonormal basis set $\left(\underline{e_r}, \underline{e_\theta}, \underline{e_1}\right)$ can also be used. In this cylindrical representation, coordinates of the position vector are denoted (r, θ, x_1). As in Hervé and Zaoui (1995), let phase (i), for $i \in \{1, 2, \ldots, n+1\}$, lie within

the shell limited by the inner radius R_{i-1} and the outer radius R_i (see Figure 1). It should be noted that we consider $R_0 = 0$ and $R_{n+1} \to \infty$. The interfaces between the different phases are supposed to be perfect leading to the continuity of the displacement vector $\underline{u}$ and of the stress vector $\underline{T}$ at each interface $r = R_i$. Let $k_{23}^{(i)}$ and $\mu_{23}^{(i)}$ be respectively the transverse bulk and shear moduli of phase (i) and $\underline{\underline{\varepsilon}}$ and $\underline{\underline{\sigma}}$ be respectively the strain and stress tensors. A cylindrical symmetry behaviour is considered where $k_{23}^{(i)}$ and $\mu_{23}^{(i)}$ depend only on r. In order to determine the effective transverse bulk and shear moduli of the assemblage (i.e. k_{23}^{eff} and μ_{23}^{eff}), two elementary loadings modes are studied: an in-plane hydrostatic mode and an in-plane transverse shear one.

2.2. Methodology

In the two studied modes the same methodology has been used in order to derive closed-form solutions of the transverse bulk and shear moduli. The local fields inside each phase of each pattern λ with $\lambda \in \{1, 2, \ldots, N_\lambda\}$ are here expressed thanks to the model developed in Hervé and Zaoui (1995) and simplified recently in Hervé-Luanco (2020). Let n_λ be the number of phases inside pattern λ and m_λ the volume fraction of pattern λ. Phase (i_λ) corresponds to the part of phase (i) present in pattern λ. Depending on the context, i_λ can take an explicit form[4] or represents the position of phase (i) inside the pattern λ using an integer to indicate the ranking. This is particularly the case if calculations are carried out with i_λ such as, for example, $i_\lambda - 1$. In that latter case, i_λ may take the following values $\{1, 2, \ldots, n_\lambda\}$. Consider that the studied material occupies a volume Ω

[4]For instance 1_2, designating phase (1) in pattern 2.

and that the volume corresponding to pattern λ is denoted Ω_λ. We suppose that $\Omega = \cup_{\lambda=1}^{N_\lambda} \Omega_\lambda$ and that $\cap_{\lambda=1}^{N_\lambda} \Omega_\lambda = \emptyset$. We also denote by Ω_i the volume corresponding to all the parts of phase (i) present in several patterns and consider that $\Omega_i = \cup_{\lambda=1}^{N_\lambda} \Omega_{i_\lambda}$ and $\cap_{\lambda=1}^{N_\lambda} \Omega_{i_\lambda} = \emptyset$ where Ω_{i_λ} is the volume corresponding to the phase (i) in pattern λ. The particular case of two patterns and two phases (section 3) makes it possible to grasp more easily the relationship between (i) and (i_λ).

Overall properties are defined through consideration of a boundary value problem. The determination of the effective behaviour is derived from first, the solution of the elementary problem of each pattern embedded in an infinite homogeneous elastic matrix with adequate moduli subjected to the same uniform strain at infinity and secondly, with some adequate average operation leading to the determination of the effective elastic stiffness tensor $\underset{\sim}{C}^{\text{eff}}$ (transverse moduli in this paper). The first step is to consider that the same kind of boundary conditions are imposed on each pattern as for the classical GSCS model (Hervé-Luanco, 2020). The terminal sections of the composite are subjected to the following boundary condition:

$$\left.\begin{array}{l} u_1^0 = 0 \\ T_2^0 = 0 \\ T_3^0 = 0 \end{array}\right\} \tag{1}$$

and the lateral surface, i.e. $r = R_{n+1}$, to the following ones:

$$\underline{u}^{\text{g}} = \underset{\sim}{E}.\,\underline{x} \tag{2}$$

276 On the terminal section of each pattern:

$$\left.\begin{array}{l} u_1^0 = 0 \\ T_2^0 = 0 \\ T_3^0 = 0 \end{array}\right\} \tag{3}$$

277 and on the lateral surface of each pattern:

$$\underline{u}^0 = \underset{\sim}{\varepsilon}^0 . \underline{x} \tag{4}$$

278 where $\underset{\sim}{\varepsilon}^0$ in Eq. (4) depends on the considered mode (in-plane hydrostatic or in-plane transverse shear mode).

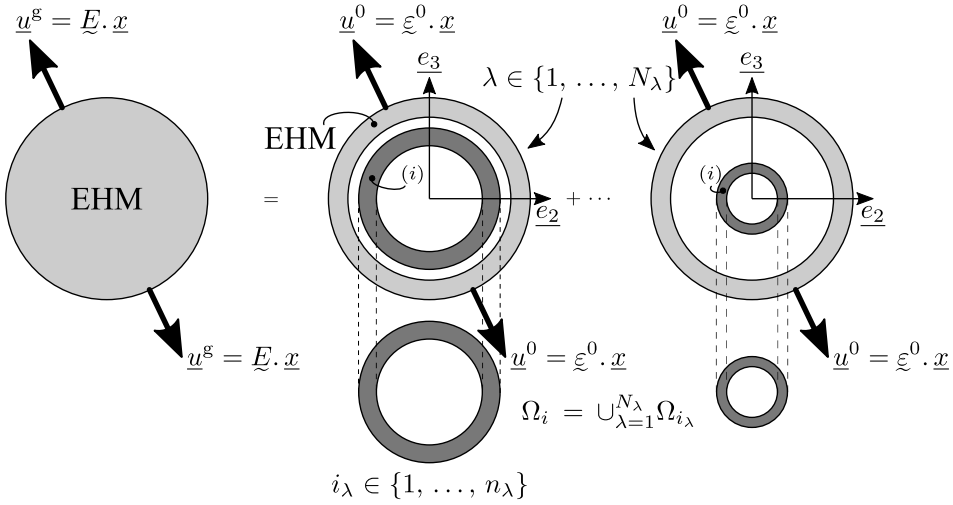

Figure 2: MRP approach with N_λ patterns made of a n_λ-layered cylindrical inclusion embedded in an infinite medium, i.e. phase $(n+1)$, also corresponding to the Equivalent Homogeneous Medium (EHM).

279

280 The linear constitutive relation for elasticity will be denoted by:

$$\underset{\sim}{\sigma} = \underset{\sim}{C} : \underset{\sim}{\varepsilon} \tag{5}$$

Since we disregard eigenstrains the average strain tensor in any phase (i) is written as follows:

$$\langle \underset{\sim}{\varepsilon} \rangle_{\Omega i} = \underset{\approx}{\mathcal{A}_i} : \underset{\sim}{E} \tag{6}$$

where $\underset{\approx}{\mathcal{A}_i}$ is the average intensity concentration tensor regarding phase (i). The effective elastic moduli tensor $\underset{\approx}{C}^{\text{eff}}$ is derived from the following relations:

$$\underset{\sim}{\Sigma} = \langle \underset{\sim}{\sigma} \rangle_{\Omega} = \underset{\approx}{C}^{\text{eff}} : \langle \underset{\sim}{\varepsilon} \rangle_{\Omega} = \underset{\approx}{C}^{\text{eff}} : \underset{\sim}{E} \tag{7}$$

It comes immediately from Eqs. (5), (Eq. (6)) and (Eq. (7)) that:

$$\underset{\sim}{\Sigma} = \left\langle \underset{\approx}{C} : \underset{\approx}{\mathcal{A}} \right\rangle_{\Omega} : \underset{\sim}{E} = \sum_{i=1}^{n} f_i \, \underset{\approx}{C}^{(i)} : \underset{\approx}{\mathcal{A}_i} : \underset{\sim}{E} \tag{8}$$

where f_i is the volume fraction of phase (i). Consequently, as defined by Hill (1963):

$$\underset{\approx}{C}^{\text{eff}} = \sum_{i=1}^{n} f_i \, \underset{\approx}{C}^{(i)} : \underset{\approx}{\mathcal{A}_i} \tag{9}$$

2.3. In-plane hydrostatic mode

In the case where an in-plane hydrostatic mode is considered, following Hervé and Zaoui (1995), $\underset{\sim}{\varepsilon}^0$ in Eq. (4) is chosen as:

$$\underset{\sim}{\varepsilon}^0 = \beta^0 \left[\left(\underline{e_2} \otimes \underline{e_2} \right) + \left(\underline{e_3} \otimes \underline{e_3} \right) \right] \tag{10}$$

Thanks to the $(n+1)$-phase problem solved in Hervé and Zaoui (1995) (Eq.[95] (37)), with $\epsilon = 0$, as typographically defined in Hervé and Zaoui's paper (1995), we know the average strain tensor $\langle \underset{\sim}{\varepsilon} \rangle_{\Omega_{i_\lambda}}$ in each phase (i_λ) of any pattern λ:

$$\langle \underset{\sim}{\varepsilon} \rangle_{\Omega_{i_\lambda}} = \frac{Q_{11}^{(i_\lambda - 1)}}{Q_{11}^{(n_\lambda)}} \beta^0 \left[(\underline{e}_2 \otimes \underline{e}_2) + (\underline{e}_3 \otimes \underline{e}_3) \right] \tag{11}$$

From Eqs. (10) and (Eq. (11)) it is worth noticing that $\langle \underset{\sim}{\varepsilon} \rangle_{\Omega_{i_\lambda}}$ can be written under the following form:

$$\langle \underset{\sim}{\varepsilon} \rangle_{\Omega_{i_\lambda}} = \mathcal{A}_{i_\lambda} \underset{\sim}{\varepsilon}^0 \tag{12}$$

where $\mathcal{A}_{i_\lambda}$ is a scalar defined by:

$$\mathcal{A}_{i_\lambda} = \frac{Q_{11}^{(i_\lambda - 1)}}{Q_{11}^{(n_\lambda)}} \tag{13}$$

and where $\boldsymbol{Q}$ is the transfer matrix defined in Hervé and Zaoui (1995). It is now possible to write the strain average of whole phase (i) (m_λ is the volume fraction of pattern λ):

$$\langle \underset{\sim}{\varepsilon} \rangle_{\Omega_i} = \sum_{\lambda=1}^{N_\lambda} m_\lambda \langle \underset{\sim}{\varepsilon} \rangle_{\Omega_{i_\lambda}} = \sum_{\lambda=1}^{N_\lambda} m_\lambda \mathcal{A}_{i_\lambda} \underset{\sim}{\varepsilon}^0 \tag{14}$$

Therefore:

$$\underset{\approx}{E} = \langle \underset{\sim}{\varepsilon} \rangle_{\Omega} = \sum_{i=1}^{n} f_i \langle \underset{\sim}{\varepsilon} \rangle_{\Omega_i} = \left[\sum_{i=1}^{n} f_i \left(\sum_{\lambda=1}^{N_\lambda} m_\lambda \mathcal{A}_{i_\lambda} \right) \right] \underset{\sim}{\varepsilon}^0 \tag{15}$$

It is worth noticing that consequently:

$$\left.\begin{aligned} \underset{\approx}{E} &= E \left[\left(\underline{e}_2 \otimes \underline{e}_2 \right) + \left(\underline{e}_3 \otimes \underline{e}_3 \right) \right] \\ \text{with} \quad E &= \left[\sum_{i=1}^{n} f_i \left(\sum_{\lambda=1}^{N_\lambda} m_\lambda \mathcal{A}_{i_\lambda} \right) \right] \beta^0 \end{aligned} \right\} \tag{16}$$

From Eqs.[95] (39) and (40) of Hervé and Zaoui (1995), with $\epsilon = 0$ and using Eq. (A.1) from Appendix A (which summarizes some basic elastic relations applied to transversely isotropic systems), we get the average stress tensor in phase (i_λ) when each pattern λ is subjected to boundary conditions defined in Eq. (4) with $\underset{\sim}{\varepsilon}^0$ given by Eq. (10):

$$\left.\begin{aligned} &\langle \sigma_{11} \rangle_{\Omega_{i_\lambda}} = 2\, C_{12}^{(i_\lambda)} \mathcal{A}_{i_\lambda} \beta^0 \\ &\langle \sigma_{22} \left(\underline{e}_2 \otimes \underline{e}_2 \right) + \sigma_{33} \left(\underline{e}_3 \otimes \underline{e}_3 \right) \rangle_{\Omega_{i_\lambda}} = 2\, k_{23}^{(i_\lambda)} \mathcal{A}_{i_\lambda} \underset{\sim}{\varepsilon}^0 \end{aligned} \right\} \tag{17}$$

leading to:

$$\left.\begin{aligned}
&\langle\sigma_{11}\rangle_\Omega = \left[\sum_{i=1}^{n} f_i \left(\sum_{\lambda=1}^{N_\lambda} m_\lambda \; 2 \; C_{12}^{(i_\lambda)} \mathcal{A}_{i_\lambda}\right)\right] \beta^0 \\
&\langle\sigma_{22}\,(\underline{e}_2 \otimes \underline{e}_2) + \sigma_{33}\,(\underline{e}_3 \otimes \underline{e}_3)\rangle_\Omega = \\
&\qquad\qquad \left[\sum_{i=1}^{n} f_i \left(\sum_{\lambda=1}^{N_\lambda} m_\lambda \; 2 \; k_{23}^{(i_\lambda)} \mathcal{A}_{i_\lambda}\right)\right] \underline{\underline{\varepsilon}}^0
\end{aligned}\right\} \tag{18}$$

The effective elastic moduli tensor $\underline{\underline{C}}^{\text{eff}}$ is derived from relation (Eq. (7)) and Eq. (A.1) applied to the equivalent homogeneous medium:

$$\left.\begin{aligned}
&\Sigma_{11} = 2\, C_{12}^{\text{eff}} E = \langle\sigma_{11}\rangle_\Omega \\
&\Sigma_{22}\,(\underline{e}_2 \otimes \underline{e}_2) + \Sigma_{33}\,(\underline{e}_3 \otimes \underline{e}_3) = 2\, k_{23}^{\text{eff}} \underline{\underline{E}} \\
&\qquad\qquad = \langle\sigma_{22}\,(\underline{e}_2 \otimes \underline{e}_2) + \sigma_{33}\,(\underline{e}_3 \otimes \underline{e}_3)\rangle_\Omega
\end{aligned}\right\} \tag{19}$$

Comparison between Eq. (19) and Eq. (18) where $\underline{\underline{E}}$ and E are given by Eq. (16) implies that:

$$\left.\begin{aligned}
C_{12}^{\text{eff}} &= \frac{\displaystyle\sum_{i=1}^{n} f_i \left(\sum_{\lambda=1}^{N_\lambda} m_\lambda \; C_{12}^{(i_\lambda)} \mathcal{A}_{i_\lambda}\right)}{\displaystyle\sum_{i=1}^{n} f_i \left(\sum_{\lambda=1}^{N_\lambda} m_\lambda \mathcal{A}_{i_\lambda}\right)} \\
k_{23}^{\text{eff}} &= \frac{\displaystyle\sum_{i=1}^{n} f_i \left(\sum_{\lambda=1}^{N_\lambda} m_\lambda \; k_{23}^{(i_\lambda)} \mathcal{A}_{i_\lambda}\right)}{\displaystyle\sum_{i=1}^{n} f_i \left(\sum_{\lambda=1}^{N_\lambda} m_\lambda \mathcal{A}_{i_\lambda}\right)}
\end{aligned}\right\} \tag{20}$$

The effective transverse bulk modulus is finally obtained by substituting $\mathcal{A}_{i_\lambda}$ from Eq. (13) in Eq. (20):

$$k_{23}^{\text{eff}} = \frac{\displaystyle\sum_{i=1}^{n} f_i \; k_{23}^{(i)} \sum_{\lambda=1}^{N_\lambda} m_\lambda \frac{Q_{11}^{(i_\lambda-1)}}{Q_{11}^{(n_\lambda)}}}{\displaystyle\sum_{i=1}^{n} f_i \sum_{\lambda=1}^{N_\lambda} m_\lambda \frac{Q_{11}^{(i_\lambda-1)}}{Q_{11}^{(n_\lambda)}}} \tag{21}$$

and we get the effective value of C_{12} in the same manner:

$$C_{12}^{\text{eff}} = \frac{\displaystyle\sum_{i=1}^{n} f_i \, C_{12}^{(i)} \sum_{\lambda=1}^{N_\lambda} m_\lambda \frac{Q_{11}^{(i_\lambda-1)}}{Q_{11}^{(n_\lambda)}}}{\displaystyle\sum_{i=1}^{n} f_i \sum_{\lambda=1}^{N_\lambda} m_\lambda \frac{Q_{11}^{(i_\lambda-1)}}{Q_{11}^{(n_\lambda)}}} \tag{22}$$

Eq. (22) will not be considered in the following because only the elastic transverse behaviour is adressed in this paper.

It should be noted that k_{23}^{eff}, given by Eq. (21), depends on the volume fraction of each phase in the composite, on the volume fraction of each pattern, on the distribution of the different phases inside each pattern and also on the transverse properties (bulk and shear moduli) of each phase.

Such a coupling between the effective moduli is totally similar to that noticed for macroscopically isotropic particulate composites by Bardella and Genna (2001).

It has been shown in Hervé-Luanco (2020) (following Eq. (23)) that $Q_{11}^{(n_\lambda)}$ depends on k_{23}^{eff} and on μ_{23}^{eff}:

$$\boldsymbol{Q}^{(n_\lambda)} = \boldsymbol{J}_{n_\lambda+1}^{-1}\left(R_{n_\lambda}\right) \boldsymbol{Q}^{*(n_\lambda)} \tag{23}$$

with

$$\boldsymbol{J}_{n_\lambda+1}^{-1}\left(R_{n_\lambda}\right) = \frac{1}{2\,R_{n_\lambda}\left(k_{23}^{(n_\lambda+1)} + \mu_{23}^{(n_\lambda+1)}\right)} \begin{pmatrix} 2\,\mu_{23}^{(n_\lambda+1)} & R_{n_\lambda} \\ 2\,k_{23}^{(n_\lambda+1)} & -R_{n_\lambda} \end{pmatrix} \tag{24}$$

leading immediately to:

$$Q_{11}^{(n_\lambda)} = \frac{2\,\mu_{23}^{(n_\lambda+1)} Q_{11}^{*(n_\lambda)} + R_{n_\lambda} Q_{21}^{*(n_\lambda)}}{2\,R_{n_\lambda}\left(k_{23}^{(n_\lambda+1)} + \mu_{23}^{(n_\lambda+1)}\right)} \tag{25}$$

k_{23}^{eff} can be rearranged by substituting Eq. (25) into Eq. (21):

$$k_{23}^{\text{eff}} = \frac{\displaystyle\sum_{i=1}^{n} f_i \, k_{23}^{(i)} \sum_{\lambda=1}^{N_\lambda} m_\lambda \frac{Q_{11}^{(i_\lambda-1)} R_{n_\lambda}}{2\,\mu_{23}^{\text{eff}} Q_{11}^{*(n_\lambda)} + R_{n_\lambda} Q_{21}^{*(n_\lambda)}}}{\displaystyle\sum_{i=1}^{n} f_i \sum_{\lambda=1}^{N_\lambda} m_\lambda \frac{Q_{11}^{(i_\lambda-1)} R_{n_\lambda}}{2\,\mu_{23}^{\text{eff}} Q_{11}^{*(n_\lambda)} + R_{n_\lambda} Q_{21}^{*(n_\lambda)}}} \tag{26}$$

where $\left(k_{23}^{(n_\lambda+1)} + \mu_{23}^{(n_\lambda+1)}\right)$ has been removed because this expression is the same in all the patterns (same infinite medium).

The different matrices $\boldsymbol{Q}$ and $\boldsymbol{Q}^*$ present in Eq. (26) depend all on the pattern λ they refer to. For this reason and in order to more easily evaluate k_{23}^{eff}, we will write it in the following form[5] using the symbol $\textcircled{\lambda}$ to denote the pattern dependency:

$$k_{23}^{\text{eff}} = \frac{\displaystyle\sum_{i=1}^{n} f_i \, k_{23}^{(i)} \sum_{\lambda=1}^{N_\lambda} m_\lambda \frac{Q_{11}^{(i_\lambda-1)\textcircled{\lambda}} R_{n_\lambda\textcircled{\lambda}}}{2\,\mu_{23}^{\text{eff}} Q_{11}^{*\textcircled{\lambda}} + R_{n_\lambda\textcircled{\lambda}} Q_{21}^{*\textcircled{\lambda}}}}{\displaystyle\sum_{i=1}^{n} f_i \sum_{\lambda=1}^{N_\lambda} m_\lambda \frac{Q_{11}^{(i_\lambda-1)\textcircled{\lambda}} R_{n_\lambda\textcircled{\lambda}}}{2\,\mu_{23}^{\text{eff}} Q_{11}^{*\textcircled{\lambda}} + R_{n_\lambda\textcircled{\lambda}} Q_{21}^{*\textcircled{\lambda}}}} \tag{27}$$

For $N_\lambda > 1$ (more than one pattern), it is worth noting that the effective transverse bulk modulus k_{23}^{eff} depends on the effective transverse shear modulus μ_{23}^{eff}.

2.4. In-plane transverse shear mode

In the case where an in-plane transverse shear mode is considered, following Hervé and Zaoui (1995), $\underset{\sim}{\varepsilon}^0$ in Eq. (4) is chosen as:

$$\underset{\sim}{\varepsilon}^0 = \gamma^0 \left[\left(\underline{e_2} \otimes \underline{e_2}\right) - \left(\underline{e_3} \otimes \underline{e_3}\right)\right] \tag{28}$$

[5] As $\boldsymbol{Q}^*$ is only written for n_λ and n_λ being perfectly defined for each pattern, $\boldsymbol{Q}^{*(n_\lambda)}$ will be equivalently written $\boldsymbol{Q}^{*\textcircled{\lambda}}$.

The same methodology as the one presented in the case of an in-plane hydrostatic mode is used.

From Eq.[95] (74) published in Hervé and Zaoui (1995), the average strain tensor $\langle \underset{\sim}{\varepsilon} \rangle_{\Omega_{i_\lambda}}$ in each phase (i_λ) of any pattern λ is given by Eq. (29), where A_{i_λ} – not to be confused with $\mathcal{A}_{i_\lambda}$ – and D_{i_λ} are defined constants for phase (i_λ) (see Hervé and Zaoui (1995)):

$$\langle \underset{\sim}{\varepsilon} \rangle_{\Omega_{i_\lambda}} = \frac{1}{D_{n_\lambda+1}} \left[D_{i_\lambda} - 3\, A_{i_\lambda} \frac{\left(R_{i_\lambda}^4 - R_{i_\lambda-1}^4 \right)}{R_{i_\lambda}^2 \left(R_{i_\lambda}^2 - R_{i_\lambda-1}^2 \right)} \right] \underset{\sim}{\varepsilon}^0 = \mathcal{A}_{i_\lambda} \underset{\sim}{\varepsilon}^0 \tag{29}$$

leading to:

$$\mathcal{A}_{i_\lambda} = \frac{1}{D_{n_\lambda+1}} \left[D_{i_\lambda} - 3\, A_{i_\lambda} \frac{\left(R_{i_\lambda}^4 - R_{i_\lambda-1}^4 \right)}{R_{i_\lambda}^2 \left(R_{i_\lambda}^2 - R_{i_\lambda-1}^2 \right)} \right] \tag{30}$$

It is easy to deduce that we have still:

$$\underset{\sim}{E} = \langle \underset{\sim}{\varepsilon} \rangle_\Omega = \sum_{i=1}^{n} f_i \langle \underset{\sim}{\varepsilon} \rangle_{\Omega_i} = \left[\sum_{i=1}^{n} f_i \left(\sum_{\lambda=1}^{N_\lambda} m_\lambda \mathcal{A}_{i_\lambda} \right) \right] \underset{\sim}{\varepsilon}^0 \tag{31}$$

with $\mathcal{A}_{i_\lambda}$ given now by Eq. (30) and consequently:

$$\left. \begin{array}{rcl} \underset{\sim}{E} & = & E \left[(\underline{e}_2 \otimes \underline{e}_2) - (\underline{e}_3 \otimes \underline{e}_3) \right] \\ \text{with} \quad E & = & \left[\sum_{i=1}^{n} f_i \left(\sum_{\lambda=1}^{N_\lambda} m_\lambda \mathcal{A}_{i_\lambda} \right) \right] \gamma^0 \end{array} \right\} \tag{32}$$

Using Eq. (A.1) we get the average stress tensor in phase (i_λ) when each pattern λ is subjected to boundary conditions defined in Eq. (4) with $\underset{\sim}{\varepsilon}^0$ given by Eq. (28):

$$\langle \underset{\sim}{\sigma} \rangle_{\Omega_{i_\lambda}} = 2\, \mu_{23}^{(i_\lambda)}\, \mathcal{A}_{i_\lambda} \underset{\sim}{\varepsilon}^0 \tag{33}$$

leading to:

$$\langle \underset{\sim}{\sigma} \rangle_\Omega = \left[\sum_{i=1}^{n} f_i \left(\sum_{\lambda=1}^{N_\lambda} m_\lambda\, 2\, \mu_{23}^{(i_\lambda)} \mathcal{A}_{i_\lambda} \right) \right] \underset{\sim}{\varepsilon}^0 \tag{34}$$

The effective elastic stiffness tensor $\underset{\approx}{C}^{\text{eff}}$ is derived from relations (Eq. (7)) and (Eq. (A.1)) applied to the equivalent homogeneous medium:

$$\underset{\approx}{\Sigma} = 2\,\mu_{23}^{\text{eff}}\underset{\approx}{E} = \langle \underset{\approx}{\sigma} \rangle_{\Omega} \tag{35}$$

Comparison between Eq. (34) and Eq. (35) (with $\underset{\approx}{\varepsilon}^0$ given by Eq. (28)), where $\underset{\approx}{E}$ and E are given by Eq. (32), implies that:

$$\mu_{23}^{\text{eff}} = \frac{\displaystyle\sum_{i=1}^{n} f_i \left(\sum_{\lambda=1}^{N_\lambda} m_\lambda\, \mu_{23}^{(i_\lambda)} \mathcal{A}_{i_\lambda} \right)}{\displaystyle\sum_{i=1}^{n} f_i \left(\sum_{\lambda=1}^{N_\lambda} m_\lambda \mathcal{A}_{i_\lambda} \right)} \tag{36}$$

Substituting Eq. (30) into Eq. (36) yields the following expression of μ_{23}^{eff}:

$$\mu_{23}^{\text{eff}} = \frac{\displaystyle\sum_{i=1}^{n} f_i\, \mu_{23}^{(i)} \sum_{\lambda=1}^{N_\lambda} m_\lambda \frac{1}{D_{n_\lambda+1}} \left[D_{i_\lambda} - 3\,A_{i_\lambda} \frac{\left(R_{i_\lambda}^4 - R_{i_\lambda-1}^4\right)}{R_{i_\lambda}^2 \left(R_{i_\lambda}^2 - R_{i_\lambda-1}^2\right)} \right]}{\displaystyle\sum_{i=1}^{n} f_i \sum_{\lambda=1}^{N_\lambda} m_\lambda \frac{1}{D_{n_\lambda+1}} \left[D_{i_\lambda} - 3\,A_{i_\lambda} \frac{\left(R_{i_\lambda}^4 - R_{i_\lambda-1}^4\right)}{R_{i_\lambda}^2 \left(R_{i_\lambda}^2 - R_{i_\lambda-1}^2\right)} \right]} \tag{37}$$

In Hervé and Zaoui (1995), the form of the solution of the displacement field is expressed in terms of four constants (A_k, B_k, C_k, D_k) in the case of a transverse shear mode and $\boldsymbol{V}_k$ denotes the matrix with these constants as components:

$$\boldsymbol{V}_k = \begin{pmatrix} A_k \\ B_k \\ C_k \\ D_k \end{pmatrix} \tag{38}$$

Here A_{i_λ} and D_{i_λ} correspond respectively to A_k and D_k and are given in Eq. (39) where phase (k) will be replaced by phase (i_λ) present in pattern λ and n will be replaced by n_λ (see Eq.[95] (72) in Hervé and Zaoui

(1995)):

$$\frac{\boldsymbol{V}_k}{D_{n+1}} = \frac{1}{Q_{44}^{(n)}Q_{11}^{(n)} - Q_{41}^{(n)}Q_{14}^{(n)}} \begin{pmatrix} Q_{11}^{(k-1)} & Q_{12}^{(k-1)} & Q_{13}^{(k-1)} & Q_{14}^{(k-1)} \\ Q_{21}^{(k-1)} & Q_{22}^{(k-1)} & Q_{23}^{(k-1)} & Q_{24}^{(k-1)} \\ Q_{31}^{(k-1)} & Q_{32}^{(k-1)} & Q_{33}^{(k-1)} & Q_{34}^{(k-1)} \\ Q_{41}^{(k-1)} & Q_{42}^{(k-1)} & Q_{43}^{(k-1)} & Q_{44}^{(k-1)} \end{pmatrix} \begin{pmatrix} -Q_{14}^{(n)} \\ 0 \\ 0 \\ Q_{11}^{(n)} \end{pmatrix} \tag{39}$$

leading to:

$$\left.\begin{aligned} \frac{A_k}{D_{n+1}} &= \frac{-Q_{11}^{(k-1)}Q_{14}^{(n)} + Q_{14}^{(k-1)}Q_{11}^{(n)}}{Q_{44}^{(n)}Q_{11}^{(n)} - Q_{41}^{(n)}Q_{14}^{(n)}} \\ \frac{D_k}{D_{n+1}} &= \frac{-Q_{14}^{(n)}Q_{41}^{(k-1)} + Q_{44}^{(k-1)}Q_{11}^{(n)}}{Q_{44}^{(n)}Q_{11}^{(n)} - Q_{41}^{(n)}Q_{14}^{(n)}} \end{aligned}\right\} \tag{40}$$

It is important to highlight that A_k, i.e. A_{i_λ} and D_k, i.e. D_{i_λ}, depend on μ_{23}^{eff} through the different components of $\boldsymbol{Q}^{(n_\lambda)}$. In order to show the dependence on μ_{23}^{eff} in Eq. (37), $\boldsymbol{Q}^{(n_\lambda)}$ is expressed thanks to Eq. (23) with $\boldsymbol{J}_{n+1}^{-1}(R_n)$ (see Hervé-Luanco (2020)) given in the transverse shear mode by:

$$\boldsymbol{J}_{n+1}^{-1}(R_n) = \frac{1}{\nu_{n+1} - 1} \begin{pmatrix} -\dfrac{R_{n+1}^2}{8\,R_n^3} & -\dfrac{R_{n+1}^2}{8\,R_n^3} & -\dfrac{R_{n+1}^2}{48\,\mu_{23}^{(n+1)}R_n^2} & -\dfrac{R_{n+1}^2}{48\,\mu_{23}^{(n+1)}R_n^2} \\ 0 & -\dfrac{R_n^3}{4\,R_{n+1}^4} & -\dfrac{\nu_{n+1}R_n^4}{12\,\mu_{23}^{(n+1)}R_{n+1}^4} & -\dfrac{(2\,\nu_{n+1}-3)R_n^4}{24\,\mu_{23}^{(n+1)}R_{n+1}^4} \\ -\dfrac{R_n}{8\,R_{n+1}^2} & \dfrac{R_n}{8\,R_{n+1}^2} & \dfrac{R_n^2}{16\,\mu_{23}^{(n+1)}R_{n+1}^2} & -\dfrac{R_n^2}{16\,\mu_{23}^{(n+1)}R_{n+1}^2} \\ -\dfrac{1}{2\,R_n} & -\dfrac{1}{4\,R_n} & \dfrac{\nu_{n+1}-1}{4\,\mu_{23}^{(n+1)}} & -\dfrac{2\,\nu_{n+1}-1}{8\,\mu_{23}^{(n+1)}} \end{pmatrix} \tag{41}$$

After tedious calculations (all the details are given in Appendix B) the final equation providing the effective shear modulus is:

$$\mu_{23}^{\text{eff}} = \frac{\displaystyle\sum_{i=1}^{n} f_i \, \mu_{23}^{(i)} \sum_{\lambda=1}^{N_\lambda} \frac{m_\lambda R_{n_\lambda \textcircled{\lambda}} \left(6 \, \mu_{23}^{\text{eff}} \alpha_{\textcircled{\lambda}}^{(i)} + R_{n_\lambda \textcircled{\lambda}} \beta_{\textcircled{\lambda}}^{(i)} \right)}{A_{\textcircled{\lambda}} \mu_{23}^{\text{eff}\,2} + B_{\textcircled{\lambda}} \mu_{23}^{\text{eff}} + C_{\textcircled{\lambda}}}}{\displaystyle\sum_{i=1}^{n} f_i \sum_{\lambda=1}^{N_\lambda} \frac{m_\lambda R_{n_\lambda \textcircled{\lambda}} \left(6 \, \mu_{23}^{\text{eff}} \alpha_{\textcircled{\lambda}}^{(i)} + R_{n_\lambda \textcircled{\lambda}} \beta_{\textcircled{\lambda}}^{(i)} \right)}{A_{\textcircled{\lambda}} \mu_{23}^{\text{eff}\,2} + B_{\textcircled{\lambda}} \mu_{23}^{\text{eff}} + C_{\textcircled{\lambda}}}} \tag{42}$$

with

$$\begin{aligned} \alpha_{\textcircled{\lambda}}^{(i)} = {} & Q_{44}^{(i_\lambda - 1)\textcircled{\lambda}} \left(Q_{11}^{*\textcircled{\lambda}} + Q_{21}^{*\textcircled{\lambda}} \right) \\ & - Q_{41}^{(i_\lambda - 1)\textcircled{\lambda}} \left(Q_{14}^{*\textcircled{\lambda}} + Q_{24}^{*\textcircled{\lambda}} \right) \\ & - 3 \, \frac{\left(R_{i_\lambda \textcircled{\lambda}}^4 - R_{i_\lambda - 1 \textcircled{\lambda}}^4 \right)}{R_{i_\lambda \textcircled{\lambda}}^2 \left(R_{i_\lambda \textcircled{\lambda}}^2 - R_{i_\lambda - 1 \textcircled{\lambda}}^2 \right)} \\ & \times \left[Q_{14}^{(i_\lambda - 1)\textcircled{\lambda}} \left(Q_{11}^{*\textcircled{\lambda}} + Q_{21}^{*\textcircled{\lambda}} \right) \right. \\ & \left. - \; Q_{11}^{(i_\lambda - 1)\textcircled{\lambda}} \left(Q_{14}^{*\textcircled{\lambda}} + Q_{24}^{*\textcircled{\lambda}} \right) \right] \end{aligned} \tag{43}$$

and

$$\begin{aligned} \beta_{\textcircled{\lambda}}^{(i)} = {} & Q_{44}^{(i_\lambda - 1)\textcircled{\lambda}} \left(Q_{31}^{*\textcircled{\lambda}} + Q_{41}^{*\textcircled{\lambda}} \right) \\ & - Q_{41}^{(i_\lambda - 1)\textcircled{\lambda}} \left(Q_{34}^{*\textcircled{\lambda}} + Q_{44}^{*\textcircled{\lambda}} \right) \\ & - 3 \, \frac{\left(R_{i_\lambda \textcircled{\lambda}}^4 - R_{i_\lambda - 1 \textcircled{\lambda}}^4 \right)}{R_{i_\lambda \textcircled{\lambda}}^2 \left(R_{i_\lambda \textcircled{\lambda}}^2 - R_{i_\lambda - 1 \textcircled{\lambda}}^2 \right)} \\ & \times \left[Q_{14}^{(i_\lambda - 1)\textcircled{\lambda}} \left(Q_{31}^{*\textcircled{\lambda}} + Q_{41}^{*\textcircled{\lambda}} \right) \right. \\ & \left. - \; Q_{11}^{(i_\lambda - 1)\textcircled{\lambda}} \left(Q_{34}^{*\textcircled{\lambda}} + Q_{44}^{*\textcircled{\lambda}} \right) \right] \end{aligned} \tag{44}$$

$A_{\textcircled{\lambda}}$, $B_{\textcircled{\lambda}}$ and $C_{\textcircled{\lambda}}$ have been determined in Eq. (B.14) of Appendix B:

$$\left.\begin{aligned} A_{\textcircled{\lambda}} &= 12\, Z_{12}^{\textcircled{\lambda}} + 6\,\frac{R_{n_\lambda \textcircled{\lambda}}}{k_{23}^{\text{eff}}}\left(Z_{14}^{\textcircled{\lambda}} + Z_{32}^{\textcircled{\lambda}} + Z_{24}^{\textcircled{\lambda}} + Z_{31}^{\textcircled{\lambda}}\right) \\ B_{\textcircled{\lambda}} &= \frac{2\, Z_{34}^{\textcircled{\lambda}} R_{n_\lambda \textcircled{\lambda}}^2}{k_{23}^{\text{eff}}} + 2\, R_{n_\lambda \textcircled{\lambda}}\left(2\, Z_{14}^{\textcircled{\lambda}} + 2 Z_{32}^{\textcircled{\lambda}} + Z_{24}^{\textcircled{\lambda}} + Z_{31}^{\textcircled{\lambda}}\right) \\ C_{\textcircled{\lambda}} &= Z_{34}^{\textcircled{\lambda}} R_{n_\lambda \textcircled{\lambda}}^2 \end{aligned}\right\} \tag{45}$$

where $Z_{ij}^{\textcircled{\lambda}}$ denotes:

$$Z_{ij}^{\textcircled{\lambda}} \overset{\text{def}}{=} Q_{i4}^{*\textcircled{\lambda}} Q_{j1}^{*\textcircled{\lambda}} - Q_{j4}^{*\textcircled{\lambda}} Q_{i1}^{*\textcircled{\lambda}} \tag{46}$$

It should be noted (see Eqs. (42) and (Eq. (45))) that the transverse shear modulus depends on the transverse bulk modulus. Finally both moduli k_{23}^{eff} and μ_{23}^{eff} are linked together. In addition, the radius $R_{n_\lambda \textcircled{\lambda}}$ disappears in both final equations (Eq. (27)) and (Eq. (42)) for particular cases of N_λ and n_λ (see section 3 for $N_\lambda = 2$ and $n_\lambda = 2$ for each pattern).

3. Particular case of two patterns with two phases in each pattern ($N_\lambda = n_\lambda = 2$)

In this section we consider one "direct" pattern and one "inverse" pattern as drawn in Figure 3.

The first pattern ($\lambda = 1$) is called the "direct" pattern and consists in two concentric cylinders where the internal phase is made of the fibre material (1) and the external phase of the pure matrix material (2). The second pattern ($\lambda = 2$) is called the "inverse" pattern and, on the opposite, the internal phase is made now of the pure matrix material (2) and the external phase of the fibre material (1). Let f be the overall volume fraction of fibre,

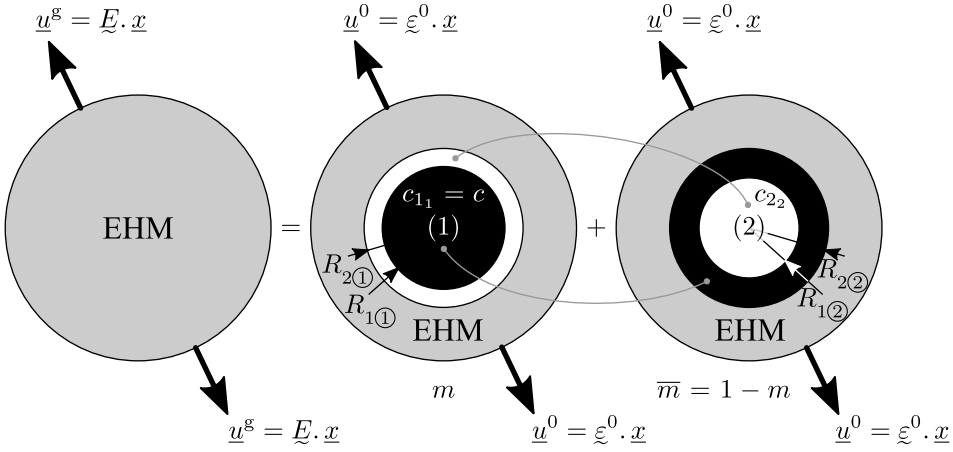

Figure 3: Two morphologically representative patterns.

i.e. $f = f_1$ and let m be the volume fraction of the first pattern and c the volume fraction of fibre inside this first pattern.

Let phase (i) $(i \in \{1, 2\})$ lie in each pattern λ within the shell limited by the two concentric cylinders with the radii $R_{i-1①}$ and $R_{i①}$ for $\lambda \in \{1, 2\}$. In this studied configuration, phase (1) represents the fibres and is split into phase (1_1) inside the direct pattern 1 and phase (1_2) inside the inverse pattern 2. As shown in Figure 3, phase (1_1) corresponds to the first phase, i.e. the internal phase of pattern 1, and lies between radii $R_{0①} = 0$ and $R_{1①}$. Still considering the fibres, phase (1_2) corresponds to the outer phase, i.e. the second phase of pattern 2, and lies between radii $R_{1②}$ and $R_{2②}$. It is important not to confuse the phase number and its indexing number within each pattern. This is expressed as follows for the volume fractions but also applies to radii: c_{i_λ} corresponds to the volume fraction of phase (i) inside pattern λ whereas $c_{i①}$ is the volume fraction of the "ith" phase inside

pattern λ; c_{2_2} and $c_{2②}$ are thus not equivalent. The parameters presented in Figure 3 are linked by the following relations:

$$\left.\begin{aligned} &c_{1_1} = c_{1①} = c = R^2_{1①}\big/R^2_{2①} \quad \text{and} \quad c_{2_1} = c_{2①} = 1 - c \\ &c_{1_2} = c_{2①} = 1 - c_{2_2} \quad \text{and} \quad c_{2_2} = c_{1②} = R^2_{1②}\big/R^2_{2②} \\ &f_1 = mc_{1_1} + (1-m)\, c_{1_2} = mc + (1-m)\,(1 - c_{2_2}) = f \\ &f_2 = 1 - f \end{aligned}\right\} \tag{47}$$

It should be noted that f, m and c are the three independent parameters of the model and all these data allow to express c_{2_2} as $c_{2_2} = [(1-f) + m\,(c-1)]/(1-m)$. Let also $k_{23}^{(i)}$ and $\mu_{23}^{(i)}$ denote respectively the plane strain bulk modulus and transverse shear modulus of phase (i).

Eq. (27) and Eq. (42) have been particularized in this particular case of two patterns with two phases in each pattern. For this purpose, the different transfer matrices $\boldsymbol{Q}$ and $\boldsymbol{Q}^*$ have been determined in Appendix C in the case of an hydrostatic pressure loading and in the case of a transverse shear loading. These developments lead to the following solution for the effective transverse modulus (see details of calculation in Appendix C.1).

$$k_{23}^{\text{eff}} \stackrel{\text{def}}{=} \frac{\underset{\subseteq k_{23}^{\text{eff}}}{\{\mathsf{C}_1\}}\mu_{23}^{\text{eff}} + \underset{\subseteq k_{23}^{\text{eff}}}{\{\mathsf{C}_2\}}}{\underset{\subseteq k_{23}^{\text{eff}}}{\{\mathsf{C}_3\}}\mu_{23}^{\text{eff}} + \underset{\subseteq k_{23}^{\text{eff}}}{\{\mathsf{C}_4\}}} \tag{48}$$

where coefficients $\underset{\subseteq k_{23}^{\text{eff}}}{\{\mathsf{C}_p\}}$ for $p \in [\![1,4]\!]$ are known in terms of the three independent parameters f, m, and c and in terms of moduli of each phase inside the two patterns (see Eq. (C.18)). With more tedious calculations the effective transverse shear modulus has been determined in Appendix

C.2 as the solution of the following equation:

$$\mu_{23}^{\text{eff}} = \overset{\curvearrowleft}{\mu_{23}^{\text{eff}}} \left(f, m, c, k_{23}^{\text{eff}}, \overset{\curvearrowright}{\mu_{23}^{\text{eff}}}, k_{23}^{(i)}, \mu_{23}^{(i)} \right) \overset{\text{def}}{=} \frac{\underset{\subseteq \mu_{23}^{\text{eff}}}{\{\mathsf{A}_1\}}}{\underset{\subseteq \mu_{23}^{\text{eff}}}{\{\mathsf{A}_2\}}} \tag{49}$$

where coefficients $\underset{\subseteq \mu_{23}^{\text{eff}}}{\{\mathsf{A}_p\}}$, $p \in [\![1, 2]\!]$, function of μ_{23}^{eff}, are defined by Eq. (C.34) and Eqs. (C.36) to (Eq. (C.44)).

4. Highlighting the usefulness of the "two patterns - two phases" approach

The specific case of two patterns with two phases in each pattern is particularly suitable for taking into account local morphological fluctuations, such as trapped matrix regions induced by the heterogeneous distribution of fibres. The purpose of this section is to illustrate this ability and to justify the addition of an inverse pattern to the classical GSCS.

In order to check the accuracy of any model, a sufficient amount of reliable "reference data" must be available. Initial resources are generally coming from experimental characterization tests and results from the literature.

A very large majority of experimental studies reported in the literature are based on "mechanical" testing techniques. Although the mechanical characterization of longitudinal and transverse Young's moduli does not, generally, provide any difficulties, this is not as simple for the characterization of the transverse bulk and shear moduli which are considered in the present paper. These moduli are usually missing from the publications and in the best case, are estimated indirectly from elastic constants easier to

obtain. To facilitate the characterization of these transverse elastics constants and reduce the inherent propagation of experimental uncertainties, alternative testing methods have been proposed.

Ultrasonic methods offer such an alternative and have been developed since the 1970's, initiated by Markham (1970) and Zimmer and Cost (1970). The principle is based on the propagation of ultrasonic waves through a sample and the phase velocity of these propagating plane waves is measured. An appropriate geometry thus makes it possible to propagate the waves in the desired directions and to estimate more easily elastic constants using the well-known Christoffel's equations. A recent review of ultrasonic methods written by Paterson et al. (2018) can be consulted for further details.

Beyond experimental results on the transverse elastic behaviour, the comparison with a micromechanical model, as presented in the present paper, requires to know the properties of the constituents but also the morphology of the microstructure. This is the case for Zimmer and Cost's paper (1970) which will allow – in a first step – to highlight that the introduction of the inverse pattern leads to better predictions of the "average" experimental values. If ultrasonic methods make it possible to limit experimental uncertainties, it nonetheless remains true that these uncertainties on average properties remain large. In addition, other problems are raised when using experimental results as reference data, even when increasing the number of tests.

Experimental results are indeed affected by behaviours unaccounted for by the linear elastic homogenization procedure, such as nonlinearities, uncertainties on the actual moduli of the employed phases, or even the presence of interphases of unknown properties between the reinforcement and

the matrix. The use of numerical experiments makes it possible to get rid of these issues. In a second step, results obtained with full-field finite element simulations are thus employed to test the present approach. Gusev et al.'s paper (2000) has been selected because it combines both experimental results – using ultrasonic techniques – and numerical ones for the desired elastic properties.

Material properties related to the two above-mentioned examples chosen to illustrate the present approach are gathered in Table 1, where "ZC" refers to Zimmer and Cost (1970), "GHW" to Gusev et al. (2000), and the superscripts "f" and "m" to the fibre and the matrix respectively. As sug-

Property & Notation		**ZC**	**GHW**	**Units**
Overall volume fraction of fibres	$\langle f \rangle$	0.49	0.54	-
Young's modulus of the fibre	$\left\langle E^{\mathrm{f}} \right\rangle$	72.4	72.5	GPa
Poisson's ratio of the fibre	$\left\langle \nu^{\mathrm{f}} \right\rangle$	0.20	0.20	-
Young's modulus of the matrix	$\langle E^{\mathrm{m}} \rangle$	4.34	5.32	GPa
Poisson's ratio of the matrix	$\langle \nu^{\mathrm{m}} \rangle$	0.36	0.365	-

Table 1: Materials data as provided by Zimmer and Cost (1970) (referred as ZC, E-glass fibre and Scotchply$^{\mathrm{TM}}$ 1002 epoxy matrix) and by Gusev et al. (2000) (referred as GHW, E-glass fibre and 913 epoxy matrix).

gested by Zimmer and Cost, due to the viscoelasticity of the resin and the ultrasonic frequencies chosen, the Young's modulus of the matrix, $\langle E^{\mathrm{m}} \rangle_{\mathrm{ZC}}$, is presented with a 40 % increase over the measured value for modelling purposes; which gave, in their situation, the best matches between experiences

and reference models. We place ourselves under the same conditions.

The primary objective of this paper is clearly the development of the model, while emphasizing its effectiveness by experimental and numerical examples [6] .

4.1. Proposed methodology

Reference data, i.e. transverse bulk and shear moduli, are firstly extracted from the two publications mentioned above (Zimmer and Cost, 1970; Gusev et al., 2000) and the uncertainties on the average values are evaluated. These results are intended to be compared with those obtained by the model presented in Section 3. For this purpose, material data from Table 1 are used as input data for the model. The transverse moduli of the unidirectional composites are derived by using an iterative algorithm – based

[6] A work in progress will complement the illustrative nature of this section and will offer to scan, different morphologies and fibre volume fractions for validation and parameter calibration purposes.

on Eqs. (C.17) and (C.33) – which can be described by Eq. (50)

$$\left.\begin{aligned}
&k_{23}^{\text{eff}} \approx k_{23}^{[j+1]} \overset{\text{def}}{=} \frac{\underset{\subseteq k_{23}^{\text{eff}}}{\{\mathsf{C}_1\}}\mu_{23}^{[j]} + \underset{\subseteq k_{23}^{\text{eff}}}{\{\mathsf{C}_2\}}}{\underset{\subseteq k_{23}^{\text{eff}}}{\{\mathsf{C}_3\}}\mu_{23}^{[j]} + \underset{\subseteq k_{23}^{\text{eff}}}{\{\mathsf{C}_4\}}} \\
&\text{with } \underset{\subseteq k_{23}^{\text{eff}}}{\{\mathsf{C}_p\}}, p \in [\![1,4]\!], \text{ depending on } \left(f, m, c, k_{23}^{(i)}, \mu_{23}^{(i)}\right) \\
&\mu_{23}^{\text{eff}} \approx \mu_{23}^{[j+1]} \overset{\text{def}}{=} \frac{\underset{\subseteq \mu_{23}^{\text{eff}}}{\{\mathsf{A}_1\}}}{\underset{\subseteq \mu_{23}^{\text{eff}}}{\{\mathsf{A}_2\}}} \\
&\text{with } \underset{\subseteq \mu_{23}^{\text{eff}}}{\{\mathsf{A}_p\}}, p \in [\![1,2]\!], \text{ depending on } \left(f, m, c, k_{23}^{(i)}, \mu_{23}^{(i)}, k_{23}^{\text{eff}} \approx k_{23}^{[j]}, \mu_{23}^{\text{eff}} \approx \mu_{23}^{[j]}\right)
\end{aligned}\right\} \quad (50)$$

and where $k_{23}^{[j]}$ and $\mu_{23}^{[j]}$ are respectively estimates of the effective plane-strain bulk and transverse shear moduli at step $[j]$, $j \in \mathbb{N}$, of the iteration process (see Figure 4). The initial estimates, $k_{23}^{[0]}$ and $\mu_{23}^{[0]}$, can be chosen as the plane-strain bulk and transverse shear moduli of the matrix or the ones of the fibre leading respectively to the lower or to the upper estimates. The iteration process is stopped when the relative error defined by Eq. (51) is lower than 10^{-6}.

$$\text{Err} = \frac{\sqrt{\left(\mu_{23}^{[j+1]} - \mu_{23}^{[j]}\right)^2 + \left(k_{23}^{[j+1]} - k_{23}^{[j]}\right)^2}}{\sqrt{\left(\mu_{23}^{[0]}\right)^2 + \left(k_{23}^{[0]}\right)^2}} \quad (51)$$

Figure 5 illustrates the iteration process for two isotropic but contrasted phases as in Hervé et al. (1991). Convergence is obtained within only a few iterations and in a fraction of a second on a personal computer.

The input parameters in Eq. (50) are the elastic behaviour of each phase and the following three morphological parameters: f, the volume fraction

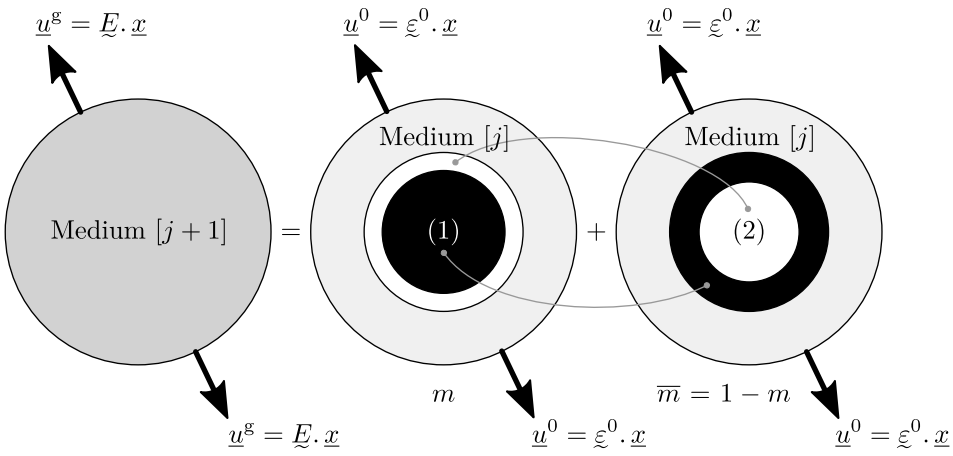

Figure 4: Recursive algorithm to get the effective transverse behaviour.

of fibre, m, the volume fraction of the "direct" pattern and c, the volume fraction of fibre inside the "direct" pattern. If the values of m and c were chosen arbitrarily in the example given in Figure 5, it is necessary to proceed differently for the comparison with Zimmer and Cost (1970) and Gusev et al. (2000) papers. Let us recall that m and c must satisfy, respectively, Eqs. (52) and (53) as in Joannès and Hervé-Luanco (2016b) .

$$m \geq \frac{1}{2} + |f - \frac{1}{2}| \tag{52}$$

$$0 \leq c_{\min} = 1 + \frac{f-1}{m} < c < c_{\max} = \frac{f}{m} \leq 1 \tag{53}$$

Knowing f from Table 1, the range of variation of m and c is determined and possible pairs (m, c) – distributed over the entire parameter space – are selected to assess the domain of the response of the model in terms of effective moduli k_{23}^{eff} and μ_{23}^{eff}. Plotting the response domain of the model makes it possible to compare it with the reference data.

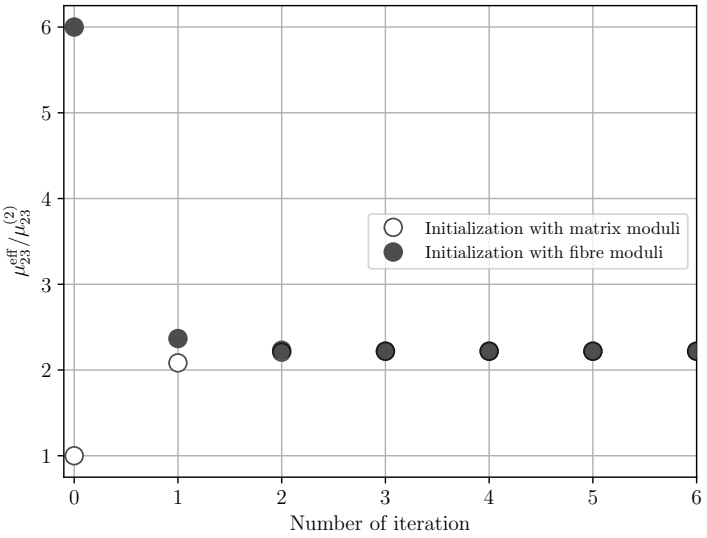

Figure 5: Effective shear modulus of a fibre-reinforced composite yielded by an iterative algorithm and normalized by the shear modulus of the matrix (phase (2)). The fibre (phase (1)) volume fraction, f, is equal to 0.5, as to m and c. Shear moduli are $\mu^{(1)} = 6$ and $\mu^{(2)} = 1$ with the Poisson's coefficients $\nu^{(1)} = 0$ and $\nu^{(2)} = 0.45$.

4.2. Results and discussion

As previously mentioned, Zimmer and Cost's paper (1970) is particularly suitable to highlight the interest of the present model. Zimmer and Cost have considered the ultrasonic characterization of a glass-epoxy composite: E-glass fibres reinforcing a Scotchply$^{\text{TM}}$ 1002 epoxy matrix (see Table 1). The following results for C_{22} and C_{23} (see Eq. (54)) have been reported with their associated uncertainties.

$$\left.\begin{aligned} \langle C_{22}\rangle_{\text{ZC}} &= (17.79 \pm 1.03)\,\text{GPa} \\ \langle C_{23}\rangle_{\text{ZC}} &= (9.79 \pm 1.52)\,\text{GPa} \end{aligned}\right\} \tag{54}$$

It is worth noting that the transverse moduli C_{22} and C_{23} are related to the effective transverse plane-strain bulk and shear moduli through Eq. (A.2). Experimental average values from Zimmer and Cost (1970) are finally given as follows:

$$\left.\begin{aligned} \left\langle k_{23}^{\text{eff}} \right\rangle_{\text{ZC}} &= (13.79 \pm 1.28)\,\text{GPa} \\ \left\langle \mu_{23}^{\text{eff}} \right\rangle_{\text{ZC}} &= (4.00 \pm 1.28)\,\text{GPa} \end{aligned}\right\} \tag{55}$$

$\left\langle k_{23}^{\text{eff}} \right\rangle_{\text{ZC}}$ is provided with an estimated uncertainty of slightly more than 9 % and $\left\langle \mu_{23}^{\text{eff}} \right\rangle_{\text{ZC}}$ with an estimated uncertainty of 32 %.

By following the iterative process described in § 4.1, and by varying m and c, it is possible to build gradually the domain of the response of the model corresponding to Zimmer and Cost's experimental results (1970). The data of Table 1 being given, for each investigated pair, (m, c), a "point" of the response domain is obtained. In order to illustrate the way the error defined in Eq. (51) decreases during the iterative algorithm, its value has been plotted in Figure 6 (top and bottom), respectively when the initial medium corresponds to the fibre (glass) and to the matrix (epoxy).

It is worth noticing that the speed of convergence, obviously for one set of parameters, is very fast; namely the number of iterations necessary to reach the desired relative error (10^{-6}) is low, i.e. 9 iterations for the conditions considered here. We have chosen to keep in Figure 6 only five different values for m with $c = f = 0.49$. This is also the case for the response domain plotted in Figure 7, even if, for this figure more values of m and c are necessary to draw the envelop curves.

Figure 7 requires some explanations; the values of k_{23}^{eff} or μ_{23}^{eff} are placed on the y-axis and evolve as a function of c (placed on the x-axis) and of m

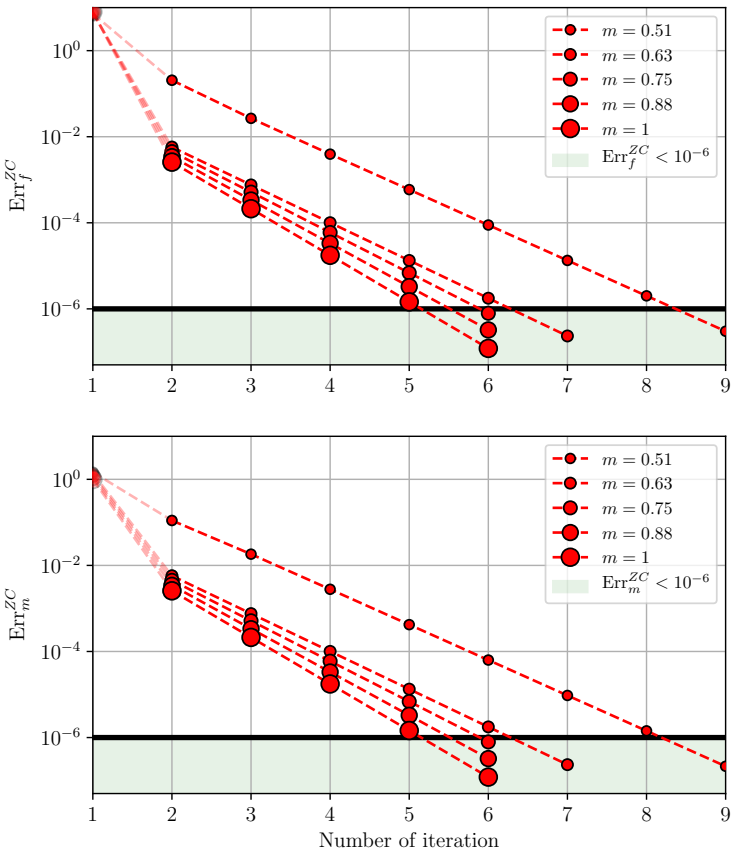

Figure 6: Error minimization during the iteration process corresponding to Zimmer and Cost's experimental conditions (1970), in the particular case where $c = f = 0.49$ and where medium [0] corresponds to the fibre (top) or to the matrix (bottom).

represented with dotted lines. The value of m is between 0.51 and 1, this latter case corresponding to the classical three-phase model (represented by the "⊙" symbol), and the limit values for c are indicated by left and right triangles. What appears first is the relatively large area related to Zimmer

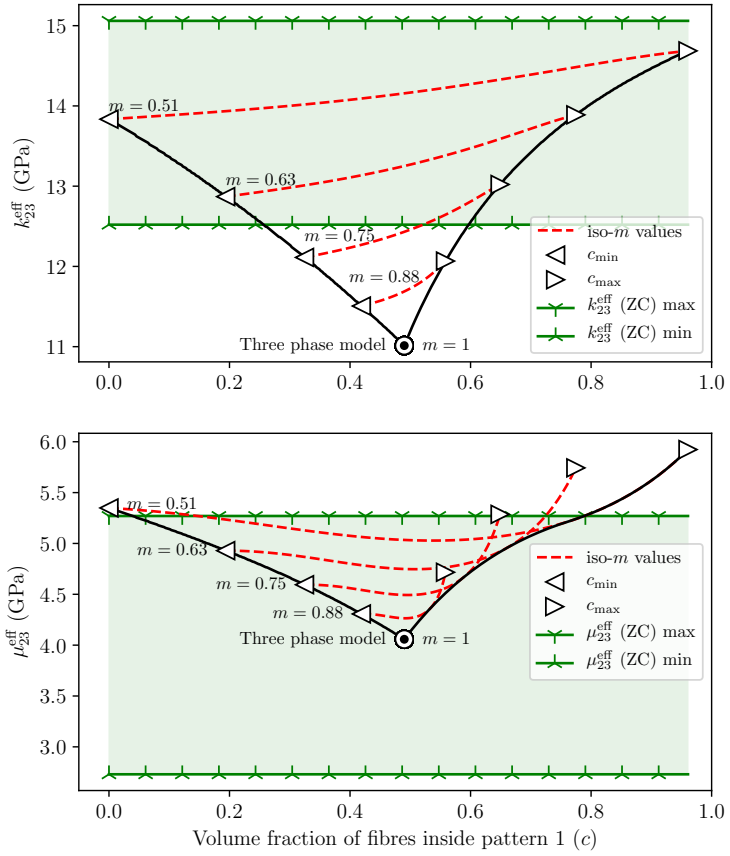

Figure 7: Analytical results, obtained with the present model, are compared to Zimmer and Cost's experimental data (1970).

and Cost's results (1970) inherent to the experimental uncertainties. If the GSCS predicted value for μ_{23}^{eff} is very close to that obtained experimentally by Zimmer and Cost, it is not the same for k_{23}^{eff}, which is far below the expected value. The response domain of the proposed model is located be-

tween the solid line curves (envelope curves). The response domain is quite large and allows to reach the plain-strain bulk modulus obtained experimentally. An infinity of pairs (m, c) achieves this goal but the experimental uncertainty is really too broad to provide further conclusions. These are the limits of this first comparison step based on experimental results.

As already stated, the second set of data is taken from Gusev et al. (2000) where a glass-epoxy composite is also considered: E-glass fibres reinforcing a 913 epoxy matrix. In Gusev et al.'s work (2000), the ultrasonic experimental results are compared to finite element simulations making it possible to overcome a large part of the uncertainty problems raised above. Elastic constants "are calculated numerically based on periodic Monte Carlo realizations with unit cells comprising a random dispersion of 100 non-overlapping fibres". According to the authors, this process is sufficient to reduce the uncertainty on the average values of elastic constants to less than 1 %. They show a good agreement between the experimental and numerical results. Thanks to their numerical approach, they also show "that the randomness of the composite microstructure had a significant influence on the transverse composite elastic constants"; what is now well known and justifies the use of the MRP approach which offers great flexibility. Gusev et al.'s numerical results (2000) are used in this second comparison step and C_{22} and C_{23} are calculated from the compliance matrix provided in their paper. The following results have been found while considering an uncertainty of 1 %:

$$\left.\begin{aligned} \langle C_{22}\rangle_{\mathrm{GWH}} &= (22.38 \pm 0.22)\,\mathrm{GPa} \\ \langle C_{23}\rangle_{\mathrm{GWH}} &= (10.09 \pm 0.10)\,\mathrm{GPa} \end{aligned}\right\} \tag{56}$$

which leads to Eq. (57) (using Eq. (A.2)) :

$$\left.\begin{aligned}\left\langle k_{23}^{\text{eff}}\right\rangle_{\text{GWH}} &= (16.23 \pm 0.16)\,\text{GPa}\\ \left\langle \mu_{23}^{\text{eff}}\right\rangle_{\text{GWH}} &= (6.14 \pm 0.16)\,\text{GPa}\end{aligned}\right\} \tag{57}$$

It is necessary to say that the value of μ_{23}^{eff} provided in Gusev et al.'s paper (2000) is slightly below (about 1 %) the value calculated here, which ensures the transverse isotropy.

As for the first step, the domain of the response of the proposed model is plotted in Figure 8. It can be seen that the analytical results are in good agreement and encompass the numerical values. However Gusev et al. do not give precise estimates of the uncertainties of their simulations, which in all cases are negligible compared to the range of values represented and are not shown in Figure 8. The three-phase model corresponding to $m = 1$ is the lowest value of the predicted moduli in Figure 7 and Figure 8, the predicted moduli are far below the expected values for the materials that are considered in this paper. This can be explained by the fact that, in the studied microstructures, a part of the matrix is trapped by the fibres (see for instance an image[7] of the transverse cross-section of Gusev et al.'s material (2000) in Figure 9).

Figure 7 and Figure 8 clearly show that the introduction of an inverse pattern makes it possible to considerably extend the prediction range of the three phase model. The reference values considered in the two comparison steps are reached without any difficulty by varying m and c. These last two figures provide a wealth of results and other analyzes can be drawn from them:

[7] A similar micrograph is presented in Zimmer and Cost's publication (1970).

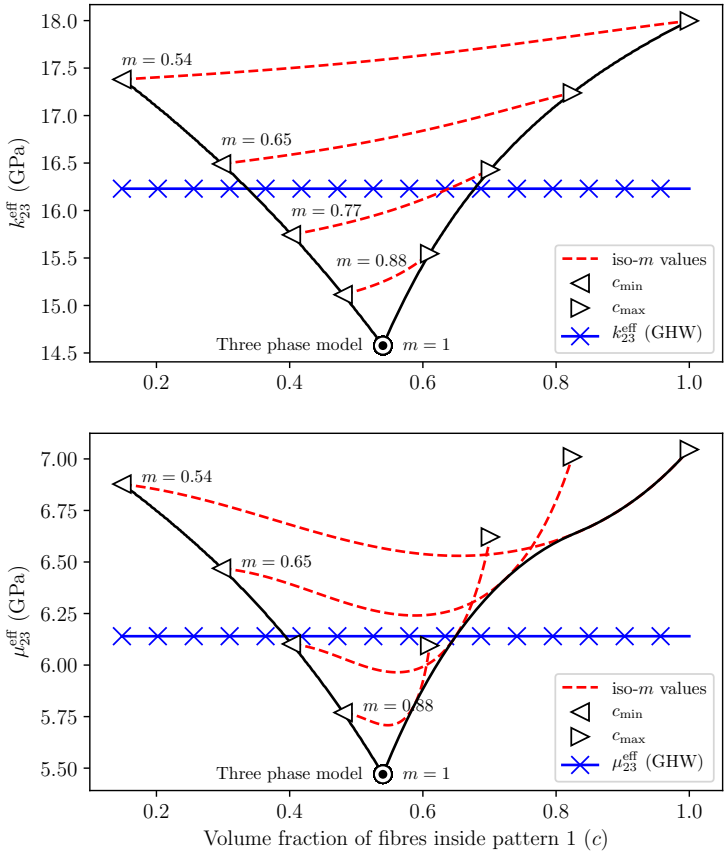

Figure 8: Analytical predicted transverse moduli compared to Gusev et al.'s numerical results (2000).

- Even considering relatively low contributions of the inverse pattern, it is possible to increase the transverse moduli by several percent. This is "graphically" highlighted in Figure 7 where the experimental uncertainty range is plotted. In the studied configuration and as a

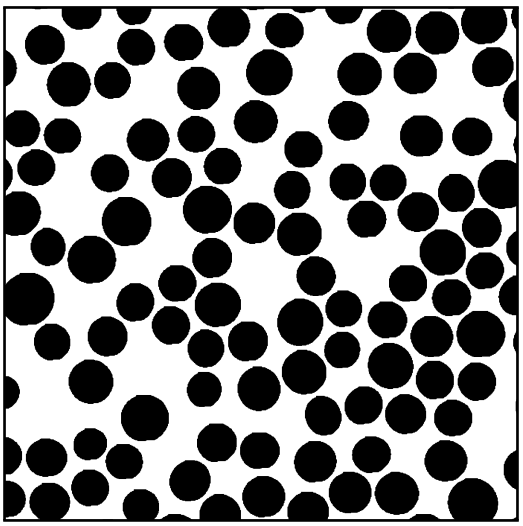

Figure 9: Example of a transverse cross-section microstructure of a unidirectional composite taken from Gusev et al. (2000). Glass fibres appears in black and the epoxy matrix in white, trapped matrix regions are clearly visible.

first approximation, considering a third of reverse pattern and two-thirds of direct pattern allows about 20 % variation on the values of k_{23}^{eff} or μ_{23}^{eff}.

- In the case of the plain strain bulk modulus, for a given $m \neq 1$, varying c does not offer much "modulation" of the predicted values.

- The effect of c is much more visible when considering the transverse shear modulus. Two areas appear in the k_{23}^{eff} graphs of Figure 7 and Figure 8: "$c < f$" and "$c > f$". When $c < f$, the sensitivity to c is very low as in the case of μ_{23}^{eff} analysed above. When $c > f$, the sensitivity to c becomes very large and tiny variations are enough to increase the predicted values by a few percent. This highly sensitive area is probably difficult to use, while providing very little added

value in terms of the predicted range.

- As a first approximation, setting $c = f$ seems to be a good modelling compromise. This allows a wide modulus range to be obtained while ensuring stability and smoothness regarding predicted values. Moreover, it seems that (m, c) solutions pairs for k_{23}^{eff} and μ_{23}^{eff} are quite close[8].

5. Conclusion

In this paper, a pattern-based method has been introduced to take into account the effect of the morphological fluctuations on the transverse elastic behaviour of fibre reinforced composites. For that purpose a Generalized Self-Consistent Scheme based on N_λ patterns with n_λ phases each has been proposed. The particular case of two patterns with two phases has been completely developed, the first pattern is a "direct" one (fibre embedded in the matrix) and the other is an "inverted" one (matrix embedded in the phase fibre). This second pattern allows us to take into account the role the non-percolated matrix part plays on the transverse elastic behaviour. Two additional morphological parameters (m, the volume fraction of the direct pattern in the microstructure and c, the volume fraction of fibre inside the second pattern) have been introduced.

As it has been shown in this paper, these two parameters make it possible to widely extend the predictive capacity of the classical three phase model. For a given microstructure, several pairs (m, c) seem to be able

[8]This analysis, dealing with the uniqueness of solution pairs, constitutes a work in progress that goes beyond the scope of the present paper.

to accurately describe the experimental results. This means that from an appropriately identified pair (m, c), it is possible to predict the transverse behaviour of a composite microstructure with trapped or non-percolated matrix areas. This identification, which is not the subject of this paper, can be carried out in different ways. An image analysis procedure, derived from a covariogram analysis can for example be applied and is under development by the authors. Moreover, a work in progress aims to show that for a given microstructure, a couple (m, c) can be chosen quasi-independently of the phase contrast and the phase properties in order to predict effective transverse elastic constants.

Acknowledgement

This study has been supported by Michelin Company. The authors are indebted to R. Bruant and A. Mbiakop-Ngassa for fruitful discussions during this work.

Appendix A. Elastic behaviour of transversely isotropic systems

The linear constitutive relation, for elasticity is written here in the form:

$$\begin{pmatrix} \sigma_{11} \equiv \sigma_1 \\ \sigma_{22} \equiv \sigma_2 \\ \sigma_{33} \equiv \sigma_3 \\ \sigma_{23} \equiv \sigma_4 \\ \sigma_{31} \equiv \sigma_5 \\ \sigma_{12} \equiv \sigma_6 \end{pmatrix} = \begin{pmatrix} C_{11} & C_{12} & C_{12} & 0 & 0 & 0 \\ C_{12} & C_{22} & C_{23} & 0 & 0 & 0 \\ C_{12} & C_{23} & C_{22} & 0 & 0 & 0 \\ 0 & 0 & 0 & C_{44} & 0 & 0 \\ 0 & 0 & 0 & 0 & C_{55} & 0 \\ 0 & 0 & 0 & 0 & 0 & C_{55} \end{pmatrix} \begin{pmatrix} \varepsilon_1 \equiv \varepsilon_{11} \\ \varepsilon_2 \equiv \varepsilon_{22} \\ \varepsilon_3 \equiv \varepsilon_{33} \\ \varepsilon_4 \equiv 2\,\varepsilon_{23} \\ \varepsilon_5 \equiv 2\,\varepsilon_{31} \\ \varepsilon_6 \equiv 2\,\varepsilon_{12} \end{pmatrix} \tag{A.1}$$

In the equivalent homogeneous material we will use C_{ij}^{eff} and in phase (k) $C_{ij}^{(k)}$ to describe their respective elastic behaviour. By combining C_{22} and C_{23}, k_{23} and μ_{23} can be calculated as follows:

$$\begin{aligned} k_{23} &= \frac{C_{22}+C_{23}}{2} \\ \mu_{23} &= \frac{C_{22}-C_{23}}{2} \end{aligned} \tag{A.2}$$

Appendix B. Determination of $\boldsymbol{\mu_{23}^{\text{eff}}}$ in the case of $\boldsymbol{N_\lambda}$ patterns with $\boldsymbol{n_\lambda}$ phases

In section 2.4, the homogenisation approach has led to the following effective transverse shear modulus (Eq. (37)):

$$\mu_{23}^{\text{eff}} = \frac{\displaystyle\sum_{i=1}^{n} f_i\, \mu_{23}^{(i)} \sum_{\lambda=1}^{N_\lambda} m_\lambda \frac{1}{D_{n_\lambda+1}} \left[D_{i_\lambda} - 3\, A_{i_\lambda} \frac{\left(R_{i_\lambda}^4 - R_{i_\lambda-1}^4\right)}{R_{i_\lambda}^2 \left(R_{i_\lambda}^2 - R_{i_\lambda-1}^2\right)} \right]}{\displaystyle\sum_{i=1}^{n} f_i \sum_{\lambda=1}^{N_\lambda} m_\lambda \frac{1}{D_{n_\lambda+1}} \left[D_{i_\lambda} - 3\, A_{i_\lambda} \frac{\left(R_{i_\lambda}^4 - R_{i_\lambda-1}^4\right)}{R_{i_\lambda}^2 \left(R_{i_\lambda}^2 - R_{i_\lambda-1}^2\right)} \right]} \tag{B.1}$$

$A_{i_\lambda}/D_{n_\lambda+1}$ and $D_{i_\lambda}/D_{n_\lambda+1}$ in Eq. (B.1) are given by Eq. (40) which is written in the following form:

$$\left.\begin{aligned} \frac{A_{i_\lambda}}{D_{n_\lambda+1}} &= \frac{Q_{14}^{(i_\lambda-1)} Q_{11}^{(n_\lambda)} - Q_{11}^{(i_\lambda-1)} Q_{14}^{(n_\lambda)}}{Q_{44}^{(n_\lambda)} Q_{11}^{(n_\lambda)} - Q_{41}^{(n_\lambda)} Q_{14}^{(n_\lambda)}} \\ \frac{D_{i\lambda}}{D_{n_\lambda+1}} &= \frac{Q_{44}^{(i_\lambda-1)} Q_{11}^{(n_\lambda)} - Q_{14}^{(n_\lambda)} Q_{41}^{(i_\lambda-1)}}{Q_{44}^{(n_\lambda)} Q_{11}^{(n_\lambda)} - Q_{41}^{(n_\lambda)} Q_{14}^{(n_\lambda)}} \end{aligned}\right\} \tag{B.2}$$

It should be noted that A_{i_λ} and D_{i_λ} depend on μ_{23}^{eff} through the different components of $\boldsymbol{Q}^{(n_\lambda)}$. In order to exhibit the dependance on μ_{23}^{eff} in Eq. (B.1), $\boldsymbol{Q}^{(n_\lambda)}$ is expressed thanks to Eq. (B.3) where $\boldsymbol{Q}^{*(n_\lambda)}$ does not depend on μ_{23}^{eff}:

$$\boldsymbol{Q}^{(n_\lambda)} = \boldsymbol{J}_{n_\lambda+1}^{-1}\left(R_{n_\lambda}\right) \boldsymbol{Q}^{*(n_\lambda)} \tag{B.3}$$

with $(\nu_{n_\lambda+1}-1)\,\boldsymbol{J}_{n_\lambda+1}^{-1}(R_{n_\lambda})$ (see Hervé-Luanco (2020)) given in the transverse shear mode by:

$$\begin{pmatrix} -\dfrac{R_{n_\lambda+1}^2}{8\,R_{n_\lambda}^3} & -\dfrac{R_{n_\lambda+1}^2}{8\,R_{n_\lambda}^3} & -\dfrac{R_{n_\lambda+1}^2}{48\,\mu_{23}^{(n_\lambda+1)}R_{n_\lambda}^2} & -\dfrac{R_{n_\lambda+1}^2}{48\,\mu_{23}^{(n_\lambda+1)}R_{n_\lambda}^2} \\ 0 & -\dfrac{R_{n_\lambda}^3}{4\,R_{n_\lambda+1}^4} & -\dfrac{\nu_{n_\lambda+1}R_{n_\lambda}^4}{12\,\mu_{23}^{(n_\lambda+1)}R_{n_\lambda+1}^4} & -\dfrac{(2\,\nu_{n_\lambda+1}-3)R_{n_\lambda}^4}{24\,\mu_{23}^{(n_\lambda+1)}R_{n_\lambda+1}^4} \\ -\dfrac{R_{n_\lambda}}{8\,R_{n_\lambda+1}^2} & \dfrac{R_{n_\lambda}}{8\,R_{n_\lambda+1}^2} & \dfrac{R_{n_\lambda}^2}{16\,\mu_{23}^{(n_\lambda+1)}R_{n_\lambda+1}^2} & -\dfrac{R_{n_\lambda}^2}{16\,\mu_{23}^{(n_\lambda+1)}R_{n_\lambda+1}^2} \\ -\dfrac{1}{2\,R_{n_\lambda}} & -\dfrac{1}{4\,R_{n_\lambda}} & \dfrac{\nu_{n_\lambda+1}-1}{4\,\mu_{23}^{(n_\lambda+1)}} & -\dfrac{2\,\nu_{n_\lambda+1}-1}{8\,\mu_{23}^{(n_\lambda+1)}} \end{pmatrix} \tag{B.4}$$

To facilitate reading, n_λ being perfectly defined for each pattern, $\boldsymbol{Q}^{*(n_\lambda)}$ will be noted $\boldsymbol{Q}^{*\textcircled{\lambda}}$ in the following equations where $\textcircled{\lambda}$ denotes the pattern dependency. It is worth taking into account that phase $(n_\lambda+1)$ is the same phase in all the patterns and corresponds to the effective medium. To determine k_{23}^{eff} and μ_{23}^{eff}, we will thus consider that $k_{23}^{\text{eff}}=k_{23}^{(n_\lambda+1)}$ and $\mu_{23}^{\text{eff}}=\mu_{23}^{(n_\lambda+1)}$. Coefficient $\nu_{n_\lambda+1}$ can be calculated by using its definition given in Hervé and Zaoui (1995):

$$\nu_{n_\lambda+1}=\frac{C_{23}^{(n_\lambda+1)}}{C_{23}^{(n_\lambda+1)}+C_{22}^{(n_\lambda+1)}} \tag{B.5}$$

By using Eq. (A.2):

$$\left.\begin{aligned} k_{23}^{(n_\lambda+1)} &= \frac{C_{22}^{(n_\lambda+1)}+C_{23}^{(n_\lambda+1)}}{2} \\ \mu_{23}^{(n_\lambda+1)} &= \frac{C_{22}^{(n_\lambda+1)}-C_{23}^{(n_\lambda+1)}}{2} \end{aligned}\right\} \tag{B.6}$$

$\nu_{n_\lambda+1}$ can then equivalently be rewritten as:

$$\nu_{n_\lambda+1}=\frac{k_{23}^{(n_\lambda+1)}-\mu_{23}^{(n_\lambda+1)}}{2\,k_{23}^{(n_\lambda+1)}} \tag{B.7}$$

Or more generally as:

$$\nu_k=\frac{k_{23}^{(k)}-\mu_{23}^{(k)}}{\frac{2}{45}\,k_{23}^{(k)}} \tag{B.8}$$

Let us now calculate the denominator of equation (Eq. (B.2)):

$$\underset{\subseteq/D_{n_\lambda+1}}{\{\mathsf{A}\}} \overset{\text{def}}{=} Q_{44}^{(n_\lambda)} Q_{11}^{(n_\lambda)} - Q_{41}^{(n_\lambda)} Q_{14}^{(n_\lambda)} \tag{B.9}$$

All of the components of $\boldsymbol{Q}^{(n_\lambda)}$ present in the previous equation can be determined by introducing Eq. (B.4) in (Eq. (B.3)):

$$\left.\begin{aligned}
Q_{44}^{(n_\lambda)} &= \frac{1}{\nu_{n_\lambda+1}-1}\left[-\frac{Q_{14}^{*(\lambda)}}{2\,R_{n_\lambda}} - \frac{Q_{24}^{*(\lambda)}}{4\,R_{n_\lambda}}\right. \\
&\qquad \left. + \frac{Q_{34}^{*(\lambda)}}{4\,\mu_{23}^{(n_\lambda+1)}}(\nu_{n_\lambda+1}-1) - \frac{Q_{44}^{*(\lambda)}}{8\,\mu_{23}^{(n_\lambda+1)}}(2\,\nu_{n_\lambda+1}-1)\right] \\
Q_{11}^{(n_\lambda)} &= \frac{1}{\nu_{n_\lambda+1}-1}\left(\frac{R_{n_\lambda+1}}{R_{n_\lambda}}\right)^2\left[-\frac{Q_{11}^{*(\lambda)}}{8\,R_{n_\lambda}}\right. \\
&\qquad \left. - \frac{Q_{21}^{*(\lambda)}}{8\,R_{n_\lambda}} - \frac{Q_{31}^{*(\lambda)}}{48\,\mu_{23}^{(n_\lambda+1)}} - \frac{Q_{41}^{*(\lambda)}}{48\,\mu_{23}^{(n_\lambda+1)}}\right] \\
Q_{41}^{(n_\lambda)} &= \frac{1}{\nu_{n_\lambda+1}-1}\left[-\frac{Q_{11}^{*(\lambda)}}{2\,R_{n_\lambda}} - \frac{Q_{21}^{*(\lambda)}}{4\,R_{n_\lambda}}\right. \\
&\qquad \left. + \frac{Q_{31}^{*(\lambda)}}{4\,\mu_{23}^{(n_\lambda+1)}}(\nu_{n_\lambda+1}-1) - \frac{Q_{41}^{*(\lambda)}}{8\,\mu_{23}^{(n_\lambda+1)}}(2\,\nu_{n_\lambda+1}-1)\right] \\
Q_{14}^{(n_\lambda)} &= \frac{1}{\nu_{n_\lambda+1}-1}\left(\frac{R_{n_\lambda+1}}{R_{n_\lambda}}\right)^2\left[-\frac{Q_{14}^{*(\lambda)}}{8\,R_{n_\lambda}}\right. \\
&\qquad \left. - \frac{Q_{24}^{*(\lambda)}}{8\,R_{n_\lambda}} - \frac{Q_{34}^{*(\lambda)}}{48\,\mu_{23}^{(n_\lambda+1)}} - \frac{Q_{44}^{*(\lambda)}}{48\,\mu_{23}^{(n_\lambda+1)}}\right]
\end{aligned}\right\} \tag{B.10}$$

Using Eqs. (B.7) and (Eq. (B.10)), $\underset{\subseteq/D_{n_\lambda+1}}{\{\mathsf{A}\}}$ can consequently be rewritten as:

$$\underset{\subseteq/D_{n_\lambda+1}}{\{\mathsf{A}\}} = \frac{4\,R_{n_\lambda+1}^2}{R_{n_\lambda}^2\left(1+\dfrac{\mu_{23}^{(n_\lambda+1)}}{k_{23}^{(n_\lambda+1)}}\right)^2}\left(\underset{\subseteq/D_{n_\lambda+1}}{\{\mathsf{B}_1\}}\ \underset{\subseteq/D_{n_\lambda+1}}{\{\mathsf{B}_2\}} - \underset{\subseteq/D_{n_\lambda+1}}{\{\mathsf{B}_3\}}\ \underset{\subseteq/D_{n_\lambda+1}}{\{\mathsf{B}_4\}}\right) \tag{B.11}$$

685 with $\underset{\subseteq/D_{n_\lambda+1}}{\{\mathsf{B}_p\}}$, $p \in [\![1,4]\!]$, given by:

$$\left.\begin{aligned}
\underset{\subseteq/D_{n_\lambda+1}}{\{\mathsf{B}_1\}} &\overset{\text{def}}{=} -\frac{Q_{14}^{*\textcircled{\lambda}}}{2\,R_{n_\lambda}} - \frac{Q_{24}^{*\textcircled{\lambda}}}{4\,R_{n_\lambda}} + \frac{Q_{34}^{*\textcircled{\lambda}}}{4\,\mu_{23}^{(n_\lambda+1)}}(\nu_{n_\lambda+1}-1) \\
&\qquad\qquad - \frac{Q_{44}^{*\textcircled{\lambda}}}{8\,\mu_{23}^{(n_\lambda+1)}}(2\,\nu_{n_\lambda+1}-1) \\
\underset{\subseteq/D_{n_\lambda+1}}{\{\mathsf{B}_2\}} &\overset{\text{def}}{=} -\frac{Q_{11}^{*\textcircled{\lambda}}}{8\,R_{n_\lambda}} - \frac{Q_{21}^{*\textcircled{\lambda}}}{8\,R_{n_\lambda}} - \frac{Q_{31}^{*\textcircled{\lambda}}}{48\,\mu_{23}^{(n_\lambda+1)}} - \frac{Q_{41}^{*\textcircled{\lambda}}}{48\,\mu_{23}^{(n_\lambda+1)}} \\
\underset{\subseteq/D_{n_\lambda+1}}{\{\mathsf{B}_3\}} &\overset{\text{def}}{=} -\frac{Q_{11}^{*\textcircled{\lambda}}}{2\,R_{n_\lambda}} - \frac{Q_{21}^{*\textcircled{\lambda}}}{4\,R_{n_\lambda}} + \frac{Q_{31}^{*\textcircled{\lambda}}}{4\,\mu_{23}^{(n_\lambda+1)}}(\nu_{n_\lambda+1}-1) \\
&\qquad\qquad - \frac{Q_{41}^{*\textcircled{\lambda}}}{8\,\mu_{23}^{(n_\lambda+1)}}(2\,\nu_{n_\lambda+1}-1) \\
\underset{\subseteq/D_{n_\lambda+1}}{\{\mathsf{B}_4\}} &\overset{\text{def}}{=} -\frac{Q_{14}^{*\textcircled{\lambda}}}{8\,R_{n_\lambda}} - \frac{Q_{24}^{*\textcircled{\lambda}}}{8\,R_{n_\lambda}} - \frac{Q_{34}^{*\textcircled{\lambda}}}{48\,\mu_{23}^{(n_\lambda+1)}} - \frac{Q_{44}^{*\textcircled{\lambda}}}{48\,\mu_{23}^{(n_\lambda+1)}}
\end{aligned}\right\} \tag{B.12}$$

By rearranging (Eq. (B.12)) thanks to $Z_{ij}^{\textcircled{\lambda}} \overset{\text{def}}{=} Q_{i4}^{*\textcircled{\lambda}} Q_{j1}^{*\textcircled{\lambda}} - Q_{j4}^{*\textcircled{\lambda}} Q_{i1}^{*\textcircled{\lambda}}$ with $i,j \in \{1,4\}$ (Eq. (46)) and by using (Eq. (B.7)) it follows that:

$$384\; R_{n_\lambda}^2 \mu_{23}^{(n_\lambda+1)^2} \left(\underset{\subseteq/D_{n_\lambda+1}}{\{\mathsf{B}_1\}} \underset{\subseteq/D_{n_\lambda+1}}{\{\mathsf{B}_2\}} - \underset{\subseteq/D_{n_\lambda+1}}{\{\mathsf{B}_3\}} \underset{\subseteq/D_{n_\lambda+1}}{\{\mathsf{B}_4\}} \right) = A_{\textcircled{\lambda}} \mu_{23}^{(n_\lambda+1)^2} + B_{\textcircled{\lambda}} \mu_{23}^{(n_\lambda+1)} + C_{\textcircled{\lambda}} \tag{B.13}$$

686 with $A_{\textcircled{\lambda}}$, $B_{\textcircled{\lambda}}$ and $C_{\textcircled{\lambda}}$ given by:

$$\left.\begin{aligned}
A_{\textcircled{\lambda}} &\overset{\text{def}}{=} 12\, Z_{12}^{\textcircled{\lambda}} + 6\,\frac{R_{n_\lambda\textcircled{\lambda}}}{k_{23}^{\text{eff}}} \left(Z_{14}^{\textcircled{\lambda}} + Z_{32}^{\textcircled{\lambda}} + Z_{24}^{\textcircled{\lambda}} + Z_{31}^{\textcircled{\lambda}} \right) \\
B_{\textcircled{\lambda}} &\overset{\text{def}}{=} \frac{2\, Z_{34}^{\textcircled{\lambda}} R_{n_\lambda\textcircled{\lambda}}^2}{k_{23}^{\text{eff}}} + 2\, R_{n_\lambda\textcircled{\lambda}} \left(2\, Z_{14}^{\textcircled{\lambda}} + 2 Z_{32}^{\textcircled{\lambda}} + Z_{24}^{\textcircled{\lambda}} + Z_{31}^{\textcircled{\lambda}} \right) \\
C_{\textcircled{\lambda}} &\overset{\text{def}}{=} Z_{34}^{\textcircled{\lambda}} R_{n_\lambda\textcircled{\lambda}}^2
\end{aligned}\right\} \tag{B.14}$$

It is important to notice that $A_{\textcircled{\lambda}}$ and $B_{\textcircled{\lambda}}$ depend on k_{23}^{eff}.

Finally:

$$\underset{\subseteq/D_{n_\lambda+1}}{\{\mathsf{A}\}} = \frac{R_{n_\lambda+1}^2}{96\ R_{n_\lambda}^4 \left(1+\dfrac{\mu_{23}^{(n_\lambda+1)}}{k_{23}^{(n_\lambda+1)}}\right)^2 {\mu_{23}^{(n_\lambda+1)}}^2 \times \left(A_{\textcircled{\lambda}}{\mu_{23}^{(n_\lambda+1)}}^2 + B_{\textcircled{\lambda}}\mu_{23}^{(n_\lambda+1)} + C_{\textcircled{\lambda}}\right)} \quad \text{(B.15)}$$

687 Eq. (B.2) takes the following form and consequently can be calculated
688 thanks to Eq. (B.15) and to Eq. (B.10):

$$\left.\begin{aligned} \frac{A_{i_\lambda}}{D_{n_\lambda+1}} &= \frac{Q_{14}^{(i_\lambda-1)}Q_{11}^{(n_\lambda)} - Q_{11}^{(i_\lambda-1)}Q_{14}^{(n_\lambda)}}{\underset{\subseteq/D_{n_\lambda+1}}{\{\mathsf{A}\}}} \\ \frac{D_{i_\lambda}}{D_{n_\lambda+1}} &= \frac{Q_{44}^{(i_\lambda-1)}Q_{11}^{(n_\lambda)} - Q_{14}^{(n_\lambda)}Q_{41}^{(i_\lambda-1)}}{\underset{\subseteq/D_{n_\lambda+1}}{\{\mathsf{A}\}}} \end{aligned}\right\} \quad \text{(B.16)}$$

689 leading to:

$$\frac{A_{i_\lambda}}{D_{n_\lambda+1}} = \frac{4\ R_{n_\lambda}\left(1+\dfrac{\mu_{23}^{(n_\lambda+1)}}{k_{23}^{(n_\lambda+1)}}\right)\left(6\ {\mu_{23}^{(n_\lambda+1)}}^2\alpha_{A_{i_\lambda}} + R_{n_\lambda}\mu_{23}^{(n_\lambda+1)}\beta_{A_{i_\lambda}}\right)}{A_{\textcircled{\lambda}}{\mu_{23}^{(n_\lambda+1)}}^2 + B_{\textcircled{\lambda}}\mu_{23}^{(n_\lambda+1)} + C_{\textcircled{\lambda}}} \quad \text{(B.17)}$$

690 with

$$\left.\begin{aligned} \alpha_{A_{i_\lambda}} &\overset{\text{def}}{=} Q_{14}^{(i_\lambda-1)}\left(Q_{11}^{*\textcircled{\lambda}} + Q_{21}^{*\textcircled{\lambda}}\right) - Q_{11}^{(i_\lambda-1)}\left(Q_{14}^{*\textcircled{\lambda}} + Q_{24}^{*\textcircled{\lambda}}\right) \\ \beta_{A_{i_\lambda}} &\overset{\text{def}}{=} Q_{14}^{(i_\lambda-1)}\left(Q_{31}^{*\textcircled{\lambda}} + Q_{41}^{*\textcircled{\lambda}}\right) - Q_{11}^{(i_\lambda-1)}\left(Q_{34}^{*\textcircled{\lambda}} + Q_{44}^{*\textcircled{\lambda}}\right) \end{aligned}\right\} \quad \text{(B.18)}$$

691 and

$$\frac{D_{i_\lambda}}{D_{n_\lambda+1}} = \frac{4\ R_{n_\lambda}\left(1+\dfrac{\mu_{23}^{(n_\lambda+1)}}{k_{23}^{(n_\lambda+1)}}\right)\left[6\ {\mu_{23}^{(n_\lambda+1)}}^2\alpha_{D_{i_\lambda}} + R_{n_\lambda}\mu_{23}^{(n_\lambda+1)}\beta_{D_{i_\lambda}}\right]}{A_{\textcircled{\lambda}}{\mu_{23}^{(n_\lambda+1)}}^2 + B_{\textcircled{\lambda}}\mu_{23}^{(n_\lambda+1)} + C_{\textcircled{\lambda}}} \quad \text{(B.19)}$$

with

$$\left.\begin{aligned}\alpha_{D_{i_\lambda}} &\stackrel{\text{def}}{=} Q_{44}^{(i_\lambda-1)}\left(Q_{11}^{*\textcircled{\lambda}}+Q_{21}^{*\textcircled{\lambda}}\right)-Q_{41}^{(i_\lambda-1)}\left(Q_{14}^{*\textcircled{\lambda}}+Q_{24}^{*\textcircled{\lambda}}\right)\\ \beta_{D_{i_\lambda}} &\stackrel{\text{def}}{=} Q_{44}^{(i_\lambda-1)}\left(Q_{31}^{*\textcircled{\lambda}}+Q_{41}^{*\textcircled{\lambda}}\right)-Q_{41}^{(i_\lambda-1)}\left(Q_{34}^{*\textcircled{\lambda}}+Q_{44}^{*\textcircled{\lambda}}\right)\end{aligned}\right\} \tag{B.20}$$

Replacing $A_{i_\lambda}/D_{n_\lambda+1}$ and $D_{i_\lambda}/D_{n_\lambda+1}$ respectively with the expressions given by Eq. (B.17) and by Eq. (B.19) in Eq. (B.1), μ_{23}^{eff} becomes:

$$\mu_{23}^{\text{eff}}=\frac{\displaystyle\sum_{i=1}^{n} f_i\,\mu_{23}^{(i)}\sum_{\lambda=1}^{N_\lambda}\frac{4\,m_\lambda R_{n_\lambda}\left(1+\dfrac{\mu_{23}^{(n_\lambda+1)}}{k_{23}^{(n_\lambda+1)}}\right)\mu_{23}^{(n_\lambda+1)}\left(6\,\mu_{23}^{(n_\lambda+1)}\alpha_{\textcircled{\lambda}}^{(i)}+R_{n_\lambda}\beta_{\textcircled{\lambda}}^{(i)}\right)}{A_{\textcircled{\lambda}}\mu_{23}^{(n_\lambda+1)^2}+B_{\textcircled{\lambda}}\mu_{23}^{(n_\lambda+1)}+C_{\textcircled{\lambda}}}}{\displaystyle\sum_{i=1}^{n} f_i\sum_{\lambda=1}^{N_\lambda}\frac{4\,m_\lambda R_{n_\lambda}\left(1+\dfrac{\mu_{23}^{(n_\lambda+1)}}{k_{23}^{(n_\lambda+1)}}\right)\mu_{23}^{(n_\lambda+1)}\left(6\,\mu_{23}^{(n_\lambda+1)}\alpha_{\textcircled{\lambda}}^{(i)}+R_{n_\lambda}\beta_{\textcircled{\lambda}}^{(i)}\right)}{A_{\textcircled{\lambda}}\mu_{23}^{(n_\lambda+1)^2}+B_{\textcircled{\lambda}}\mu_{23}^{(n_\lambda+1)}+C_{\textcircled{\lambda}}}} \tag{B.21}$$

with

$$\left.\begin{aligned}\alpha_{\textcircled{\lambda}}^{(i)} &\stackrel{\text{def}}{=} \alpha_{D_{i_\lambda}}-3\,\frac{R_{i_\lambda}^4-R_{i_\lambda-1}^4}{R_{i_\lambda}^2\left(R_{i_\lambda}^2-R_{i_\lambda-1}^2\right)}\,\alpha_{A_{i_\lambda}}\\ \beta_{\textcircled{\lambda}}^{(i)} &\stackrel{\text{def}}{=} \beta_{D_{i_\lambda}}-3\,\frac{R_{i_\lambda}^4-R_{i_\lambda-1}^4}{R_{i_\lambda}^2\left(R_{i_\lambda}^2-R_{i_\lambda-1}^2\right)}\,\beta_{A_{i_\lambda}}\end{aligned}\right\} \tag{B.22}$$

$\mu_{23}^{(n_\lambda+1)}$ and $k_{23}^{(n_\lambda+1)}$ do not depend on the pattern they are attached to (see Figure 2) consequently they do not depend on λ and Eq. (B.21) can be rewritten as:

$$\mu_{23}^{\text{eff}}=\frac{\displaystyle\sum_{i=1}^{n} f_i\,\mu_{23}^{(i)}\sum_{\lambda=1}^{N_\lambda}\frac{m_\lambda R_{n_\lambda}\left(6\,\mu_{23}^{\text{eff}}\alpha_{\textcircled{\lambda}}^{(i)}+R_{n_\lambda}\beta_{\textcircled{\lambda}}^{(i)}\right)}{A_{\textcircled{\lambda}}\mu_{23}^{\text{eff}^2}+B_{\textcircled{\lambda}}\mu_{23}^{\text{eff}}+C_{\textcircled{\lambda}}}}{\displaystyle\sum_{i=1}^{n} f_i\sum_{\lambda=1}^{N_\lambda}\frac{m_\lambda R_{n_\lambda}\left(6\,\mu_{23}^{\text{eff}}\alpha_{\textcircled{\lambda}}^{(i)}+R_{n_\lambda}\beta_{\textcircled{\lambda}}^{(i)}\right)}{A_{\textcircled{\lambda}}\mu_{23}^{\text{eff}^2}+B_{\textcircled{\lambda}}\mu_{23}^{\text{eff}}+C_{\textcircled{\lambda}}}} \tag{B.23}$$

where

$$\left.\begin{aligned}
\alpha_{\textcircled{\lambda}}^{(i)} &= Q_{44}^{(i_\lambda-1)}\left(Q_{11}^{*\textcircled{\lambda}}+Q_{21}^{*\textcircled{\lambda}}\right)\\
&\quad -Q_{41}^{(i_\lambda-1)}\left(Q_{14}^{*\textcircled{\lambda}}+Q_{24}^{*\textcircled{\lambda}}\right)\\
&\quad -3\,\frac{\left(R_{i_\lambda}^4-R_{i_\lambda-1}^4\right)}{R_{i_\lambda}^2\left(R_{i_\lambda}^2-R_{i_\lambda-1}^2\right)}\\
&\quad \times\left[Q_{14}^{(i_\lambda-1)}\left(Q_{11}^{*\textcircled{\lambda}}+Q_{21}^{*\textcircled{\lambda}}\right)\right.\\
&\quad \left.-\;Q_{11}^{(i_\lambda-1)}\left(Q_{14}^{*\textcircled{\lambda}}+Q_{24}^{*\textcircled{\lambda}}\right)\right]\\
\beta_{\textcircled{\lambda}}^{(i)} &= Q_{44}^{(i_\lambda-1)}\left(Q_{31}^{*\textcircled{\lambda}}+Q_{41}^{*\textcircled{\lambda}}\right)\\
&\quad -Q_{41}^{(i_\lambda-1)}\left(Q_{34}^{*\textcircled{\lambda}}+Q_{44}^{*\textcircled{\lambda}}\right)\\
&\quad -3\,\frac{\left(R_{i_\lambda}^4-R_{i_\lambda-1}^4\right)}{R_{i_\lambda}^2\left(R_{i_\lambda}^2-R_{i_\lambda-1}^2\right)}\\
&\quad \times\left[Q_{14}^{(i_\lambda-1)}\left(Q_{31}^{*\textcircled{\lambda}}+Q_{41}^{*\textcircled{\lambda}}\right)\right.\\
&\quad \left.-\;Q_{11}^{(i_\lambda-1)}\left(Q_{34}^{*\textcircled{\lambda}}+Q_{44}^{*\textcircled{\lambda}}\right)\right]
\end{aligned}\right\} \tag{B.24}$$

It is worth remembering that Eq. (B.23) is an implicit equation depending both on μ_{23}^{eff} and on k_{23}^{eff} through $A_{\textcircled{\lambda}}$ and $B_{\textcircled{\lambda}}$. In the different applications we will use the following expressions to take into account the fact that the different radii and the matrices $\boldsymbol{Q}$ and $\boldsymbol{Q}^*$ present in Eq. (B.23) depend on the pattern λ they are attached to:

$$\mu_{23}^{\text{eff}}=\frac{\displaystyle\sum_{i=1}^{n}f_i\,\mu_{23}^{(i)}\sum_{\lambda=1}^{N_\lambda}\frac{m_\lambda R_{n_\lambda\textcircled{\lambda}}\left(6\,\mu_{23}^{\text{eff}}\alpha_{\textcircled{\lambda}}^{(i)}+R_{n_\lambda\textcircled{\lambda}}\beta_{\textcircled{\lambda}}^{(i)}\right)}{A_{\textcircled{\lambda}}\mu_{23}^{\text{eff}\,2}+B_{\textcircled{\lambda}}\mu_{23}^{\text{eff}}+C_{\textcircled{\lambda}}}}{\displaystyle\sum_{i=1}^{n}f_i\sum_{\lambda=1}^{N_\lambda}\frac{m_\lambda R_{n_\lambda\textcircled{\lambda}}\left(6\,\mu_{23}^{\text{eff}}\alpha_{\textcircled{\lambda}}^{(i)}+R_{n_\lambda\textcircled{\lambda}}\beta_{\textcircled{\lambda}}^{(i)}\right)}{A_{\textcircled{\lambda}}\mu_{23}^{\text{eff}\,2}+B_{\textcircled{\lambda}}\mu_{23}^{\text{eff}}+C_{\textcircled{\lambda}}}} \tag{B.25}$$

where finally

$$\left.\begin{array}{rl}
\alpha_{\textcircled{\lambda}}^{(i)} & = Q_{44}^{(i_\lambda-1)\textcircled{\lambda}}\left(Q_{11}^{*\textcircled{\lambda}}+Q_{21}^{*\textcircled{\lambda}}\right) \\
& -Q_{41}^{(i_\lambda-1)\textcircled{\lambda}}\left(Q_{14}^{*\textcircled{\lambda}}+Q_{24}^{*\textcircled{\lambda}}\right) \\
& -3\,\dfrac{\left(R_{i_\lambda\textcircled{\lambda}}^{4}-R_{i_\lambda-1\textcircled{\lambda}}^{4}\right)}{R_{i_\lambda\textcircled{\lambda}}^{2}\left(R_{i_\lambda\textcircled{\lambda}}^{2}-R_{i_\lambda-1\textcircled{\lambda}}^{2}\right)} \\
& \times\left[Q_{14}^{(i_\lambda-1)\textcircled{\lambda}}\left(Q_{11}^{*\textcircled{\lambda}}+Q_{21}^{*\textcircled{\lambda}}\right)\right. \\
& \left.-\;Q_{11}^{(i_\lambda-1)\textcircled{\lambda}}\left(Q_{14}^{*\textcircled{\lambda}}+Q_{24}^{*\textcircled{\lambda}}\right)\right] \\
\beta_{\textcircled{\lambda}}^{(i)} & = Q_{44}^{(i_\lambda-1)\textcircled{\lambda}}\left(Q_{31}^{*\textcircled{\lambda}}+Q_{41}^{*\textcircled{\lambda}}\right) \\
& -Q_{41}^{(i_\lambda-1)\textcircled{\lambda}}\left(Q_{34}^{*\textcircled{\lambda}}+Q_{44}^{*\textcircled{\lambda}}\right) \\
& -3\,\dfrac{\left(R_{i_\lambda\textcircled{\lambda}}^{4}-R_{i_\lambda-1\textcircled{\lambda}}^{4}\right)}{R_{i_\lambda\textcircled{\lambda}}^{2}\left(R_{i_\lambda\textcircled{\lambda}}^{2}-R_{i_\lambda-1\textcircled{\lambda}}^{2}\right)} \\
& \times\left[Q_{14}^{(i_\lambda-1)\textcircled{\lambda}}\left(Q_{31}^{*\textcircled{\lambda}}+Q_{41}^{*\textcircled{\lambda}}\right)\right. \\
& \left.-\;Q_{11}^{(i_\lambda-1)\textcircled{\lambda}}\left(Q_{34}^{*\textcircled{\lambda}}+Q_{44}^{*\textcircled{\lambda}}\right)\right]
\end{array}\right\} \qquad \text{(B.26)}$$

Appendix C. Details of the calculations made in the particular case of 2 patterns with 2 inverted phases

In this section a configuration with two patterns is considered, one is a "direct" pattern and the other is an "inverse" one, each one being made of two phases ($n = 2$, $N_\lambda = 2$ and $n_\lambda = 2$ for each pattern) see description in section 3 and Figure 3.

In the following, we will use the functions and parameters defined below:

$$\begin{array}{rccl}
\mathrm{Id}: & \underset{\subseteq\Omega}{\{1,2\}} & \rightarrow & \underset{\subseteq\mathbb{N}}{\{1,2\}} \\
& \lambda & \mapsto & \mathrm{Id}\,(\lambda)\;\equiv\boxed{\lambda}=\left\{\begin{array}{ll} 1 & \text{if } \lambda=1 \\ 2 & \text{if } \lambda=2 \end{array}\right.
\end{array} \qquad \text{(C.1)}$$

$$\begin{aligned} \mathrm{Cp}: \ \underset{\subseteq\Omega}{\{1,2\}} &\rightarrow \underset{\subseteq\mathbb{N}}{\{1,2\}} \\ \lambda &\mapsto \mathrm{Cp}\left(\lambda\right) \equiv \blacksquare\!\!\lambda = \begin{cases} 1 & \text{if } \lambda = 2 \\ 2 & \text{if } \lambda = 1 \end{cases} \end{aligned} \tag{C.2}$$

where the codomain $\underset{\subseteq\mathbb{N}}{\{1,2\}}$ of Id and Cp transformations have totally lost any "pattern" reference. It means that images $\mathrm{Id}\left(\lambda\right)$, i.e. $\boxed{\lambda}$, and $\mathrm{Cp}\left(\lambda\right)$, i.e. $\blacksquare\!\!\lambda$, are just natural numbers and can, for example, describe phase numbers if they are placed in parentheses or in indices as for : $\bullet^{(k)}$ or $\bullet_k$. So, taken from Hervé and Zaoui (1995):

$$\left.\begin{aligned} \rho_{\boxed{\lambda}} &\overset{\text{def}}{=} \mu_{23}^{(\boxed{\lambda})} \Big/ \mu_{23}^{(\blacksquare\!\!\lambda)} \\ a_{\boxed{\lambda}} &\overset{\text{def}}{=} \rho_{\boxed{\lambda}} + \left(3 - 4\,\nu_{\boxed{\lambda}}\right) \\ b_{\boxed{\lambda}} &\overset{\text{def}}{=} \left(3 - 2\,\nu_{\boxed{\lambda}}\right) + \rho_{\boxed{\lambda}}\left(2\,\nu_{\blacksquare\!\!\lambda} - 3\right) \\ c_{\boxed{\lambda}} &\overset{\text{def}}{=} 1 + \rho_{\boxed{\lambda}}\left(3 - 4\,\nu_{\blacksquare\!\!\lambda}\right) \\ d_{\boxed{\lambda}} &\overset{\text{def}}{=} 2\,\nu_{\boxed{\lambda}} - 1 + \rho_{\boxed{\lambda}}\left(1 - 2\,\nu_{\blacksquare\!\!\lambda}\right) \\ e_{\boxed{\lambda}} &\overset{\text{def}}{=} 1 - \rho_{\boxed{\lambda}} \end{aligned}\right\} \tag{C.3}$$

see Eq. (B.8) for $\nu_{\boxed{\lambda}}$ and $\nu_{\blacksquare\!\!\lambda}$. And:

$$q^2_{\textcircled{\lambda}} \overset{\text{def}}{=} R^2_{1\textcircled{\lambda}} \Big/ R^2_{2\textcircled{\lambda}} \ \Rightarrow \ \begin{cases} {q_{\textcircled{1}}}^2 = c \\ {q_{\textcircled{2}}}^2 = c_{2_2} \end{cases} \tag{C.4}$$

To calculate $\alpha^{(i)}_{\textcircled{\lambda}}$ and $\beta^{(i)}_{\textcircled{\lambda}}$ in the case of the determination of the effective transverse shear modulus it may be noted that:

$$c_{\boxed{\lambda}} = a_{\boxed{\lambda}} + 2\,d_{\boxed{\lambda}} \tag{C.5}$$

Appendix C.1. Development of k_{23}^{eff}

In the case of two patterns with two phases each, Eq. (27) becomes:

$$k_{23}^{\text{eff}} = \frac{\displaystyle\sum_{i=1}^{2} f_i \; k_{23}^{(i)} \sum_{\lambda=1}^{2} m_\lambda \frac{Q_{11}^{(i_\lambda-1)\textcircled{\lambda}} R_{2\textcircled{\lambda}}}{2\;\mu_{23}^{\text{eff}} Q_{11}^{*\textcircled{\lambda}} + R_{2\textcircled{\lambda}} Q_{21}^{*\textcircled{\lambda}}}}{\displaystyle\sum_{i=1}^{2} f_i \sum_{\lambda=1}^{2} m_\lambda \frac{Q_{11}^{(i_\lambda-1)\textcircled{\lambda}} R_{2\textcircled{\lambda}}}{2\;\mu_{23}^{\text{eff}} Q_{11}^{*\textcircled{\lambda}} + R_{2\textcircled{\lambda}} Q_{21}^{*\textcircled{\lambda}}}} \tag{C.6}$$

Substituting the different components of the $\boldsymbol{Q}^{\textcircled{\lambda}}$ matrices (see Hervé and Zaoui (1995)) (for $\lambda \in \{1,2\}$) in Eq. (C.6) gives:

$$k_{23}^{\text{eff}} = \frac{f k_{23}^{(1)} \underset{\subseteq k_{23}^{\text{eff}}}{\{\mathsf{A}_1\}} + (1-f)\, k_{23}^{(2)} \underset{\subseteq k_{23}^{\text{eff}}}{\{\mathsf{A}_2\}}}{f \underset{\subseteq k_{23}^{\text{eff}}}{\{\mathsf{A}_1\}} + (1-f) \underset{\subseteq k_{23}^{\text{eff}}}{\{\mathsf{A}_2\}}} \overset{\text{def}}{=} \frac{\underset{\subseteq k_{23}^{\text{eff}}}{\{\mathsf{B}_1\}}}{\underset{\subseteq k_{23}^{\text{eff}}}{\{\mathsf{B}_2\}}} \tag{C.7}$$

where

$$\left.\begin{aligned} \underset{\subseteq k_{23}^{\text{eff}}}{\{\mathsf{A}_1\}} &\overset{\text{def}}{=} \frac{m Q_{11}^{(0)\textcircled{1}} R_{2\textcircled{1}}}{2\;\mu_{23}^{\text{eff}} Q_{11}^{*\textcircled{1}} + R_{2\textcircled{1}} Q_{21}^{*\textcircled{1}}} + \frac{(1-m)\, Q_{11}^{(1)\textcircled{2}} R_{2\textcircled{2}}}{2\;\mu_{23}^{\text{eff}} Q_{11}^{*\textcircled{2}} + R_{2\textcircled{2}} Q_{21}^{*\textcircled{2}}} \\ \underset{\subseteq k_{23}^{\text{eff}}}{\{\mathsf{A}_2\}} &\overset{\text{def}}{=} \frac{m Q_{11}^{(1)\textcircled{1}} R_{2\textcircled{1}}}{2\;\mu_{23}^{\text{eff}} Q_{11}^{*\textcircled{1}} + R_{2\textcircled{1}} Q_{21}^{*\textcircled{1}}} + \frac{(1-m)\, Q_{11}^{(0)\textcircled{2}} R_{2\textcircled{2}}}{2\;\mu_{23}^{\text{eff}} Q_{11}^{*\textcircled{2}} + R_{2\textcircled{2}} Q_{21}^{*\textcircled{2}}} \end{aligned}\right\} \tag{C.8}$$

The $\boldsymbol{Q}^{\textcircled{\lambda}}$ matrices are determined from Hervé and Zaoui (1995) for $\lambda \in \{1,2\}$:

$$\boldsymbol{Q}^{(0)\textcircled{\lambda}} = \boldsymbol{I} \Longrightarrow Q_{11}^{(0)\textcircled{\lambda}} = 1 \tag{C.9}$$

$$\boldsymbol{Q}^{(1)\textcircled{\lambda}} = \boldsymbol{N}^{\lambda(1)} = \frac{1}{\mu_{23}^{(\blacksquare\!\lambda)} + k_{23}^{(\blacksquare\!\lambda)}} \begin{pmatrix} (\mu_{23}^{(\blacksquare\!\lambda)} + k_{23}^{(\boxed{\lambda})}) & \dfrac{R_{0\textcircled{\lambda}}^2}{R_{1\textcircled{\lambda}}^2}(\mu_{23}^{(\blacksquare\!\lambda)} - \mu_{23}^{(\boxed{\lambda})}) \\ (k_{23}^{(\blacksquare\!\lambda)} - k_{23}^{(\boxed{\lambda})}) & \dfrac{R_{0\textcircled{\lambda}}^2}{R_{1\textcircled{\lambda}}^2}(\mu_{23}^{(\boxed{\lambda})} + k_{23}^{(\blacksquare\!\lambda)}) \end{pmatrix} \tag{C.10}$$

$R_{0\textcircled{\lambda}}^2 = 0$ by definition leading to:

$$Q_{11}^{(1)\textcircled{\lambda}} = \frac{\mu_{23}^{(\blacksquare\!\lambda)} + k_{23}^{(\boxed{\lambda})}}{\mu_{23}^{(\blacksquare\!\lambda)} + k_{23}^{(\blacksquare\!\lambda)}} \tag{C.11}$$

In order to determine k_{23}^{eff} in terms of μ_{23}^{eff} from Eq. (C.6) the $\boldsymbol{Q}$ matrices have to be calculated by using the $\boldsymbol{Q}^*$ matrices like in Hervé-Luanco (2020).

$$\boldsymbol{Q}^{*\textcircled{\lambda}} = \boldsymbol{J}_2^{\textcircled{\lambda}}\left(R_{2\textcircled{\lambda}}\right)\boldsymbol{Q}^{(1)\textcircled{\lambda}} \tag{C.12}$$

with

$$\boldsymbol{J}_2^{\textcircled{\lambda}}\left(R_{2\textcircled{\lambda}}\right) = \begin{pmatrix} R_{2\textcircled{\lambda}} & \dfrac{R_{1\textcircled{\lambda}}^2}{R_{2\textcircled{\lambda}}} \\ 2\,k_{23}^{(\boldsymbol{\lambda})} & -2\,\dfrac{R_{1\textcircled{\lambda}}^2}{R_{2\textcircled{\lambda}}^2}\mu_{23}^{(\boldsymbol{\lambda})} \end{pmatrix} \tag{C.13}$$

It can easily been shown that:

$$\left.\begin{aligned} Q_{11}^{*\textcircled{\lambda}} &= \frac{R_{2\textcircled{\lambda}}\left(\mu_{23}^{(\boldsymbol{\lambda})} + k_{23}^{(\boxed{\lambda})}\right) + \dfrac{R_{1\textcircled{\lambda}}^2}{R_{2\textcircled{\lambda}}}\left(k_{23}^{(\boldsymbol{\lambda})} - k_{23}^{(\boxed{\lambda})}\right)}{\mu_{23}^{(\boldsymbol{\lambda})} + k_{23}^{(\boldsymbol{\lambda})}} \\ Q_{21}^{*\textcircled{\lambda}} &= \frac{2\,k_{23}^{(\boldsymbol{\lambda})}\left(\mu_{23}^{(\boldsymbol{\lambda})} + k_{23}^{(\boxed{\lambda})}\right) - 2\,\dfrac{R_{1\textcircled{\lambda}}^2}{R_{2\textcircled{\lambda}}^2}\mu_{23}^{(\boldsymbol{\lambda})}\left(k_{23}^{(\boldsymbol{\lambda})} - k_{23}^{(\boxed{\lambda})}\right)}{\mu_{23}^{(\boldsymbol{\lambda})} + k_{23}^{(\boldsymbol{\lambda})}} \end{aligned}\right\} \tag{C.14}$$

$\underset{\subseteq k_{23}^{\text{eff}}}{\{\mathsf{A}_p\}}$, $p \in [\![1,2]\!]$, in Eq. (C.8) are then written as:

$$\left.\begin{aligned} \underset{\subseteq k_{23}^{\text{eff}}}{\{\mathsf{A}_1\}} &= \frac{m\left(\mu_{23}^{(2)} + k_{23}^{(2)}\right)}{2\,\left(\mu_{23}^{(2)} + k_{23}^{(1)}\right)\left(\mu_{23}^{\text{eff}} + k_{23}^{(2)}\right) + 2\,c\,\left(k_{23}^{(2)} - k_{23}^{(1)}\right)\left(\mu_{23}^{\text{eff}} - \mu_{23}^{(2)}\right)} \\ &\quad + \frac{(1-m)\left(\mu_{23}^{(1)} + k_{23}^{(2)}\right)}{2\,\left(\mu_{23}^{(1)} + k_{23}^{(2)}\right)\left(\mu_{23}^{\text{eff}} + k_{23}^{(1)}\right) + 2\,c_{2_2}\left(k_{23}^{(1)} - k_{23}^{(2)}\right)\left(\mu_{23}^{\text{eff}} - \mu_{23}^{(1)}\right)} \\ \underset{\subseteq k_{23}^{\text{eff}}}{\{\mathsf{A}_2\}} &= \frac{m\left(\mu_{23}^{(2)} + k_{23}^{(1)}\right)}{2\,\left(\mu_{23}^{(2)} + k_{23}^{(1)}\right)\left(\mu_{23}^{\text{eff}} + k_{23}^{(2)}\right) + 2\,c\,\left(k_{23}^{(2)} - k_{23}^{(1)}\right)\left(\mu_{23}^{\text{eff}} - \mu_{23}^{(2)}\right)} \\ &\quad + \frac{(1-m)\left(\mu_{23}^{(1)} + k_{23}^{(1)}\right)}{2\,\left(\mu_{23}^{(1)} + k_{23}^{(2)}\right)\left(\mu_{23}^{\text{eff}} + k_{23}^{(1)}\right) + 2\,c_{2_2}\left(k_{23}^{(1)} - k_{23}^{(2)}\right)\left(\mu_{23}^{\text{eff}} - \mu_{23}^{(1)}\right)} \end{aligned}\right\} \tag{C.15}$$

By reintroducing $\underset{\subseteq k_{23}^{\text{eff}}}{\{\mathsf{A}_1\}}$ and $\underset{\subseteq k_{23}^{\text{eff}}}{\{\mathsf{A}_2\}}$ from Eq. (C.15) in Eq. (C.7) we obtain:

$$\left.\begin{aligned}
\underset{\subseteq k_{23}^{\text{eff}}}{\{\mathsf{B}_1\}} &= \frac{f k_{23}^{(1)} m \left(\mu_{23}^{(2)} + k_{23}^{(2)}\right) + (1-f)\, k_{23}^{(2)} m \left(\mu_{23}^{(2)} + k_{23}^{(1)}\right)}{\left(\mu_{23}^{(2)} + k_{23}^{(1)}\right)\left(\mu_{23}^{\text{eff}} + k_{23}^{(2)}\right) + c\,\left(k_{23}^{(2)} - k_{23}^{(1)}\right)\left(\mu_{23}^{\text{eff}} - \mu_{23}^{(2)}\right)} \\
&+ \frac{f k_{23}^{(1)} (1-m) \left(\mu_{23}^{(1)} + k_{23}^{(2)}\right) + (1-f)\, k_{23}^{(2)} (1-m) \left(\mu_{23}^{(1)} + k_{23}^{(1)}\right)}{\left(\mu_{23}^{(1)} + k_{23}^{(2)}\right)\left(\mu_{23}^{\text{eff}} + k_{23}^{(1)}\right) + c_{2_2}\left(k_{23}^{(1)} - k_{23}^{(2)}\right)\left(\mu_{23}^{\text{eff}} - \mu_{23}^{(1)}\right)} \\
\underset{\subseteq k_{23}^{\text{eff}}}{\{\mathsf{B}_2\}} &= \frac{f m \left(\mu_{23}^{(2)} + k_{23}^{(2)}\right) + (1-f)\, m \left(\mu_{23}^{(2)} + k_{23}^{(1)}\right)}{\left(\mu_{23}^{(2)} + k_{23}^{(1)}\right)\left(\mu_{23}^{\text{eff}} + k_{23}^{(2)}\right) + c\,\left(k_{23}^{(2)} - k_{23}^{(1)}\right)\left(\mu_{23}^{\text{eff}} - \mu_{23}^{(2)}\right)} \\
&+ \frac{f (1-m) \left(\mu_{23}^{(1)} + k_{23}^{(2)}\right) + (1-f)\, (1-m) \left(\mu_{23}^{(1)} + k_{23}^{(1)}\right)}{\left(\mu_{23}^{(1)} + k_{23}^{(2)}\right)\left(\mu_{23}^{\text{eff}} + k_{23}^{(1)}\right) + c_{2_2}\left(k_{23}^{(1)} - k_{23}^{(2)}\right)\left(\mu_{23}^{\text{eff}} - \mu_{23}^{(1)}\right)}
\end{aligned}\right\} \tag{C.16}$$

k_{23}^{eff} can finally be developed in terms of μ_{23}^{eff}:

$$k_{23}^{\text{eff}} = \frac{\underset{\subseteq k_{23}^{\text{eff}}}{\{\mathsf{C}_1\}} \mu_{23}^{\text{eff}} + \underset{\subseteq k_{23}^{\text{eff}}}{\{\mathsf{C}_2\}}}{\underset{\subseteq k_{23}^{\text{eff}}}{\{\mathsf{C}_3\}} \mu_{23}^{\text{eff}} + \underset{\subseteq k_{23}^{\text{eff}}}{\{\mathsf{C}_4\}}} \tag{C.17}$$

with

$$
\begin{aligned}
\underset{\subseteq k_{23}^{\text{eff}}}{\{\mathsf{C}_1\}} &\stackrel{\text{def}}{=} \left[f k_{23}^{(1)} m \left(\mu_{23}^{(2)} + k_{23}^{(2)}\right) + (1-f)\, k_{23}^{(2)} m \left(\mu_{23}^{(2)} + k_{23}^{(1)}\right)\right] \\
&\quad \times \left[c_{2_2} \left(k_{23}^{(1)} - k_{23}^{(2)}\right) + \left(\mu_{23}^{(1)} + k_{23}^{(2)}\right)\right] \\
&\quad + \left[f k_{23}^{(1)} (1-m) \left(\mu_{23}^{(1)} + k_{23}^{(2)}\right) + (1-f)\, k_{23}^{(2)} (1-m) \left(\mu_{23}^{(1)} + k_{23}^{(1)}\right)\right] \\
&\quad \times \left[c\ \left(k_{23}^{(2)} - k_{23}^{(1)}\right) + \left(\mu_{23}^{(2)} + k_{23}^{(1)}\right)\right] \\
\\
\underset{\subseteq k_{23}^{\text{eff}}}{\{\mathsf{C}_2\}} &\stackrel{\text{def}}{=} \left[f k_{23}^{(1)} m \left(\mu_{23}^{(2)} + k_{23}^{(2)}\right) + (1-f)\, k_{23}^{(2)} m \left(\mu_{23}^{(2)} + k_{23}^{(1)}\right)\right] \\
&\quad \times \left[\left(\mu_{23}^{(1)} + k_{23}^{(2)}\right) k_{23}^{(1)} - c_{2_2} \left(k_{23}^{(1)} - k_{23}^{(2)}\right) \mu_{23}^{(1)}\right] \\
&\quad + \left[f k_{23}^{(1)} (1-m) \left(\mu_{23}^{(1)} + k_{23}^{(2)}\right) + (1-f)\, k_{23}^{(2)} (1-m) \left(\mu_{23}^{(1)} + k_{23}^{(1)}\right)\right] \\
&\quad \times \left[\left(\mu_{23}^{(2)} + k_{23}^{(1)}\right) k_{23}^{(2)} - c\ \left(k_{23}^{(2)} - k_{23}^{(1)}\right) \mu_{23}^{(2)}\right] \\
\\
\underset{\subseteq k_{23}^{\text{eff}}}{\{\mathsf{C}_3\}} &\stackrel{\text{def}}{=} \left[f m \left(\mu_{23}^{(2)} + k_{23}^{(2)}\right) + (1-f)\, m \left(\mu_{23}^{(2)} + k_{23}^{(1)}\right)\right] \\
&\quad \times \left[c_{2_2} \left(k_{23}^{(1)} - k_{23}^{(2)}\right) + \left(\mu_{23}^{(1)} + k_{23}^{(2)}\right)\right] \\
&\quad + \left[f\, (1-m) \left(\mu_{23}^{(1)} + k_{23}^{(2)}\right) + (1-f)\, (1-m) \left(\mu_{23}^{(1)} + k_{23}^{(1)}\right)\right] \\
&\quad \times \left[c\ \left(k_{23}^{(2)} - k_{23}^{(1)}\right) + \left(\mu_{23}^{(2)} + k_{23}^{(1)}\right)\right] \\
\\
\underset{\subseteq k_{23}^{\text{eff}}}{\{\mathsf{C}_4\}} &\stackrel{\text{def}}{=} \left[f m \left(\mu_{23}^{(2)} + k_{23}^{(2)}\right) + (1-f)\, m \left(\mu_{23}^{(2)} + k_{23}^{(1)}\right)\right] \\
&\quad \times \left[\left(\mu_{23}^{(1)} + k_{23}^{(2)}\right) k_{23}^{(1)} - c_{2_2} \left(k_{23}^{(1)} - k_{23}^{(2)}\right) \mu_{23}^{(1)}\right] \\
&\quad + \left[f\, (1-m) \left(\mu_{23}^{(1)} + k_{23}^{(2)}\right) + (1-f)\, (1-m) \left(\mu_{23}^{(1)} + k_{23}^{(1)}\right)\right] \\
&\quad \times \left[\left(\mu_{23}^{(2)} + k_{23}^{(1)}\right) k_{23}^{(2)} - c\ \left(k_{23}^{(2)} - k_{23}^{(1)}\right) \mu_{23}^{(2)}\right]
\end{aligned}
\tag{C.18}
$$

Appendix C.2. Development of μ_{23}^{eff}

In the context of two patterns with two phases Eq. (42) becomes:

$$\mu_{23}^{\text{eff}} = \frac{\displaystyle\sum_{i=1}^{2} f_i \, \mu_{23}^{(i)} \sum_{\lambda=1}^{2} \frac{m_\lambda R_{2\textcircled{\lambda}} \left(6 \, \mu_{23}^{\text{eff}} \alpha_{\textcircled{\lambda}}^{(i)} + R_{2\textcircled{\lambda}} \beta_{\textcircled{\lambda}}^{(i)}\right)}{A_{\textcircled{\lambda}} \mu_{23}^{\text{eff}^2} + B_{\textcircled{\lambda}} \mu_{23}^{\text{eff}} + C_{\textcircled{\lambda}}}}{\displaystyle\sum_{i=1}^{2} f_i \sum_{\lambda=1}^{2} \frac{m_\lambda R_{2\textcircled{\lambda}} \left(6 \, \mu_{23}^{\text{eff}} \alpha_{\textcircled{\lambda}}^{(i)} + R_{2\textcircled{\lambda}} \beta_{\textcircled{\lambda}}^{(i)}\right)}{A_{\textcircled{\lambda}} \mu_{23}^{\text{eff}^2} + B_{\textcircled{\lambda}} \mu_{23}^{\text{eff}} + C_{\textcircled{\lambda}}}} \tag{C.19}$$

In order to calculate $A_{\textcircled{\lambda}} \mu_{23}^{\text{eff}^2} + B_{\textcircled{\lambda}} \mu_{23}^{\text{eff}} + C_{\textcircled{\lambda}}$ let us use the following equations:

$$\left.\begin{aligned} A_{\textcircled{\lambda}} &= 12 \, Z_{12}^{\textcircled{\lambda}} + 6 \, \frac{R_{2\textcircled{\lambda}}}{k_{23}^{\text{eff}}} \left(Z_{14}^{\textcircled{\lambda}} + Z_{32}^{\textcircled{\lambda}} + Z_{24}^{\textcircled{\lambda}} + Z_{31}^{\textcircled{\lambda}}\right) \\ B_{\textcircled{\lambda}} &= \frac{2 \, Z_{34}^{\textcircled{\lambda}} R_{2\textcircled{\lambda}}^2}{k_{23}^{\text{eff}}} + 2 \, R_{2\textcircled{\lambda}} \left(2 \, Z_{14}^{\textcircled{\lambda}} + 2 \, Z_{32}^{\textcircled{\lambda}} + Z_{24}^{\textcircled{\lambda}} + Z_{31}^{\textcircled{\lambda}}\right) \\ C_{\textcircled{\lambda}} &= Z_{34}^{\textcircled{\lambda}} R_{2\textcircled{\lambda}}^2 \end{aligned}\right\} \tag{C.20}$$

where all the Z_{ij} (see Eq.[95] (81) in Hervé and Zaoui (1995)) are already defined by:

$$Z_{ij}^{\textcircled{\lambda}} \overset{\text{def}}{=} Q_{i4}^{*\textcircled{\lambda}} Q_{j1}^{*\textcircled{\lambda}} - Q_{j4}^{*\textcircled{\lambda}} Q_{i1}^{*\textcircled{\lambda}} \tag{C.21}$$

with:

$$\boldsymbol{Q}^{*\textcircled{\lambda}} = \boldsymbol{J}_2^{\textcircled{\lambda}} \left(R_{2\textcircled{\lambda}}\right) \boldsymbol{Q}^{(1)\textcircled{\lambda}} \tag{C.22}$$

From Hervé and Zaoui (1995), in the case of a transverse shear loading,

747 $\boldsymbol{J}_2^{\textcircled{\lambda}}\left(R_{2\textcircled{\lambda}}\right)$ is given by:

$$\boldsymbol{J}_2^{\textcircled{\lambda}}\left(R_{2\textcircled{\lambda}}\right) = \begin{pmatrix} -4\,\nu_{\blacksquare} R_{2\textcircled{\lambda}} & R_{2\textcircled{\lambda}} & 4\,\left(1-\nu_{\blacksquare}\right) R_{2\textcircled{\lambda}} & R_{2\textcircled{\lambda}} \\ \left(6-4\,\nu_{\blacksquare}\right) R_{2\textcircled{\lambda}} & R_{2\textcircled{\lambda}} & -\left(2-4\,\nu_{\blacksquare}\right) R_{2\textcircled{\lambda}} & -R_{2\textcircled{\lambda}} \\ 0 & -6\,\mu_{23}^{(\blacksquare)} & -8\,\mu_{23}^{(\blacksquare)} & 2\,\mu_{23}^{(\blacksquare)} \\ 12\,\mu_{23}^{(\blacksquare)} & -6\,\mu_{23}^{(\blacksquare)} & -4\,\mu_{23}^{(\blacksquare)} & -2\,\mu_{23}^{(\blacksquare)} \end{pmatrix} \tag{C.23}$$

and $\boldsymbol{Q}^{(1)\textcircled{\lambda}}$ by:

$$\boldsymbol{Q}^{(1)\textcircled{\lambda}} = \frac{1}{4\,\left(1-\nu_{\blacksquare}\right)} \times \begin{pmatrix} \frac{a_{\boxed{\lambda}}}{q_{\textcircled{\lambda}}^2} & \frac{1-\rho_{\boxed{\lambda}}}{q_{\textcircled{\lambda}}^2} & \frac{1-\rho_{\boxed{\lambda}}}{q_{\textcircled{\lambda}}^2} & 0 \\ 2\,q_{\textcircled{\lambda}}^4 b_{\boxed{\lambda}} & q_{\textcircled{\lambda}}^4 c_{\boxed{\lambda}} & 2\,q_{\textcircled{\lambda}}^4 d_{\boxed{\lambda}} & q_{\textcircled{\lambda}}^4\left(\rho_{\boxed{\lambda}}-1\right) \\ -3\,q_{\textcircled{\lambda}}^2\left(1-\rho_{\boxed{\lambda}}\right) & 0 & q_{\textcircled{\lambda}}^2 a_{\boxed{\lambda}} & q_{\textcircled{\lambda}}^2\left(1-\rho_{\boxed{\lambda}}\right) \\ -6\,d_{\boxed{\lambda}} & 3\,\left(1-\rho_{\boxed{\lambda}}\right) & 2\,b_{\boxed{\lambda}} & c_{\boxed{\lambda}} \end{pmatrix} \tag{C.24}$$

748 The different $\boldsymbol{Q}^{*\textcircled{\lambda}}$ matrices are calculated from Eq. (C.22) with the help

of Eq. (C.23) and Eq. (C.24):

$$\left.\begin{aligned}
Q_{11}^{*\textcircled{\lambda}} &= \frac{R_{2\textcircled{\lambda}}}{4\ \left(1-\nu_{\blacksquare}\right)}\left[-4\ \nu_{\blacksquare}\frac{a_{\boxed{\lambda}}}{q_{\textcircled{\lambda}}^2}+2\ q_{\textcircled{\lambda}}^4 b_{\boxed{\lambda}}\right.\\
&\qquad\left.-12\ \left(1-\nu_{\blacksquare}\right)q_{\textcircled{\lambda}}^2 e_{\boxed{\lambda}}-6\ d_{\boxed{\lambda}}\right]\\
Q_{21}^{*\textcircled{\lambda}} &= \frac{R_{2\textcircled{\lambda}}}{4\ \left(1-\nu_{\blacksquare}\right)}\left[\left(6-4\ \nu_{\blacksquare}\right)\frac{a_{\boxed{\lambda}}}{q_{\textcircled{\lambda}}^2}+2\ q_{\textcircled{\lambda}}^4 b_{\boxed{\lambda}}\right.\\
&\qquad\left.+3\ \left(2-4\ \nu_{\blacksquare}\right)q_{\textcircled{\lambda}}^2 e_{\boxed{\lambda}}+6\ d_{\boxed{\lambda}}\right]\\
Q_{31}^{*\textcircled{\lambda}} &= \frac{2\ \mu_{23}^{(\blacksquare)}}{4\ \left(1-\nu_{\blacksquare}\right)}\left[-6\ q_{\textcircled{\lambda}}^4 b_{\boxed{\lambda}}+12\ q_{\textcircled{\lambda}}^2 e_{\boxed{\lambda}}-6\ d_{\boxed{\lambda}}\right]\\
Q_{41}^{*\textcircled{\lambda}} &= \frac{2\ \mu_{23}^{(\blacksquare)}}{4\ \left(1-\nu_{\blacksquare}\right)}\left[6\ \frac{a_{\boxed{\lambda}}}{q_{\textcircled{\lambda}}^2}-6\ q_{\textcircled{\lambda}}^4 b_{\boxed{\lambda}}+6\ q_{\textcircled{\lambda}}^2 e_{\boxed{\lambda}}+6\ d_{\boxed{\lambda}}\right]\\
Q_{14}^{*\textcircled{\lambda}} &= \frac{R_{2\textcircled{\lambda}}}{4\ \left(1-\nu_{\blacksquare}\right)}\left[-q_{\textcircled{\lambda}}^4 e_{\boxed{\lambda}}+4\ \left(1-\nu_{\blacksquare}\right)q_{\textcircled{\lambda}}^2 e_{\boxed{\lambda}}+c_{\boxed{\lambda}}\right]\\
Q_{24}^{*\textcircled{\lambda}} &= \frac{R_{2\textcircled{\lambda}}}{4\ \left(1-\nu_{\blacksquare}\right)}\left[-q_{\textcircled{\lambda}}^4 e_{\boxed{\lambda}}-\left(2-4\ \nu_{\blacksquare}\right)q_{\textcircled{\lambda}}^2 e_{\boxed{\lambda}}-c_{\boxed{\lambda}}\right]\\
Q_{34}^{*\textcircled{\lambda}} &= \frac{2\ \mu_{23}^{(\blacksquare)}}{4\ \left(1-\nu_{\blacksquare}\right)}\left[3\ q_{\textcircled{\lambda}}^4 e_{\boxed{\lambda}}-4\ q_{\textcircled{\lambda}}^2 e_{\boxed{\lambda}}+c_{\boxed{\lambda}}\right]\\
Q_{44}^{*\textcircled{\lambda}} &= \frac{2\ \mu_{23}^{(\blacksquare)}}{4\ \left(1-\nu_{\blacksquare}\right)}\left[3\ q_{\textcircled{\lambda}}^4 e_{\boxed{\lambda}}-2\ q_{\textcircled{\lambda}}^2 e_{\boxed{\lambda}}-c_{\boxed{\lambda}}\right]
\end{aligned}\right\} \tag{C.25}$$

The different components $Z_{ij}^{\textcircled{\lambda}}$ present in Eq. (C.20) can then be determined thanks to Eq. (C.21) with the previous values of $\boldsymbol{Q}^{*\textcircled{\lambda}}$ leading to:

$$\begin{aligned}
Z_{12}^{\textcircled{\lambda}} &= \frac{R_{2\textcircled{\lambda}}^2}{16\ \left(1-\nu_{\blacksquare}\right)^2}\left[-6\ q_{\textcircled{\lambda}}^2 a_{\boxed{\lambda}} e_{\boxed{\lambda}}-6\ q_{\textcircled{\lambda}}^2 e_{\boxed{\lambda}} c_{\boxed{\lambda}}+12\ q_{\textcircled{\lambda}}^2 d_{\boxed{\lambda}} e_{\boxed{\lambda}}\right.\\
&+4\ q_{\textcircled{\lambda}}^6 b_{\boxed{\lambda}} e_{\boxed{\lambda}}\left(3-4\ \nu_{\blacksquare}\right)+6\ q_{\textcircled{\lambda}}^6 e_{\boxed{\lambda}}^2\left(4\ \nu_{\blacksquare}-3\right)+4\ q_{\textcircled{\lambda}}^4 b_{\boxed{\lambda}} c_{\boxed{\lambda}}\\
&\left.-12\ q_{\textcircled{\lambda}}^4 e_{\boxed{\lambda}} d_{\boxed{\lambda}}+\frac{2\ a_{\boxed{\lambda}} c_{\boxed{\lambda}}}{q_{\textcircled{\lambda}}^2}\left(3-4\ \nu_{\blacksquare}\right)+8\ a_{\boxed{\lambda}} e_{\boxed{\lambda}}\left(3-6\ \nu_{\blacksquare}+4\ \nu_{\blacksquare}^2\right)\right]
\end{aligned} \tag{C.26}$$

$$Z_{31}^{\textcircled{\lambda}} = \frac{2\,\mu_{23}^{(\blacksquare)} R_{2\textcircled{\lambda}}}{16\,\left(1-\nu_{\blacksquare}\right)^2}\Big[8\,q_{\textcircled{\lambda}}^4 b_{\boxed{\lambda}} c_{\boxed{\lambda}} + 8\,q_{\textcircled{\lambda}}^6 e_{\boxed{\lambda}} b_{\boxed{\lambda}}\left(2-3\,\nu_{\blacksquare}\right)$$
$$-12\,q_{\textcircled{\lambda}}^2 e_{\boxed{\lambda}} c_{\boxed{\lambda}}\left(2-\nu_{\blacksquare}\right) - 12\,q_{\textcircled{\lambda}}^2 a_{\boxed{\lambda}} e_{\boxed{\lambda}}\nu_{\blacksquare} + 12\,q_{\textcircled{\lambda}}^6 e_{\boxed{\lambda}}^2\left(3\,\nu_{\blacksquare}-2\right)$$
$$+24\,q_{\textcircled{\lambda}}^2 e_{\boxed{\lambda}} d_{\boxed{\lambda}}\left(2-\nu_{\blacksquare}\right) - \frac{4\,a_{\boxed{\lambda}} c_{\boxed{\lambda}}\nu_{\blacksquare}}{q_{\textcircled{\lambda}}^2} - 24\,q_{\textcircled{\lambda}}^4 d_{\boxed{\lambda}} e_{\boxed{\lambda}} + 16\,\nu_{\blacksquare} e_{\boxed{\lambda}} a_{\boxed{\lambda}}\Big] \tag{C.27}$$

$$Z_{32}^{\textcircled{\lambda}} = \frac{2\,\mu_{23}^{(\blacksquare)} R_{2\textcircled{\lambda}}}{16\,\left(1-\nu_{\blacksquare}\right)^2}\Big[3\,\left(6-4\,\nu_{\blacksquare}\right) q_{\textcircled{\lambda}}^2 a_{\boxed{\lambda}} e_{\boxed{\lambda}} + 6\,q_{\textcircled{\lambda}}^6 e_{\boxed{\lambda}}^2\left(5-6\,\nu_{\blacksquare}\right)$$
$$-8\,\left(3-2\,\nu_{\blacksquare}\right) a_{\boxed{\lambda}} e_{\boxed{\lambda}} - 4\,\left(5-6\,\nu_{\blacksquare}\right) q_{\textcircled{\lambda}}^6 e_{\boxed{\lambda}} b_{\boxed{\lambda}}$$
$$-12\,\left(3-2\,\nu_{\blacksquare}\right) q_{\textcircled{\lambda}}^2 e_{\boxed{\lambda}} d_{\boxed{\lambda}} + \frac{2\,a_{\boxed{\lambda}} c_{\boxed{\lambda}}}{q_{\textcircled{\lambda}}^2}\left(3-2\,\nu_{\blacksquare}\right)$$
$$-4\,q_{\textcircled{\lambda}}^4 b_{\boxed{\lambda}} c_{\boxed{\lambda}} + 6\,q_{\textcircled{\lambda}}^2 c_{\boxed{\lambda}} e_{\boxed{\lambda}}\left(3-2\,\nu_{\blacksquare}\right) + 12\,q_{\textcircled{\lambda}}^4 e_{\boxed{\lambda}} d_{\boxed{\lambda}}\Big] \tag{C.28}$$

$$Z_{14}^{\textcircled{\lambda}} = \frac{2\,\mu_{23}^{(\blacksquare)} R_{2\textcircled{\lambda}}}{16\,\left(1-\nu_{\blacksquare}\right)^2}\Big[6\,\left(2\,\nu_{\blacksquare}-1\right) q_{\textcircled{\lambda}}^2 a_{\boxed{\lambda}} e_{\boxed{\lambda}} + 6\,q_{\textcircled{\lambda}}^6 e_{\boxed{\lambda}}^2\left(5-6\,\nu_{\blacksquare}\right)$$
$$+12\,q_{\textcircled{\lambda}}^4 e_{\boxed{\lambda}} d_{\boxed{\lambda}} + 8\,(3-4\,\nu_{\blacksquare}) a_{\boxed{\lambda}} e_{\boxed{\lambda}}$$
$$+4\,q_{\textcircled{\lambda}}^6 b_{\boxed{\lambda}} e_{\boxed{\lambda}}\left(6\,\nu_{\blacksquare}-5\right) + 12\,\left(1-2\,\nu_{\blacksquare}\right) q_{\textcircled{\lambda}}^2 d_{\boxed{\lambda}} e_{\boxed{\lambda}}$$
$$+\frac{2\,a_{\boxed{\lambda}} c_{\boxed{\lambda}}}{q_{\textcircled{\lambda}}^2}(3-2\,\nu_{\blacksquare}) - 4\,q_{\textcircled{\lambda}}^4 b_{\boxed{\lambda}} c_{\boxed{\lambda}} + 6\,(2\,\nu_{\blacksquare}-1) q_{\textcircled{\lambda}}^2 e_{\boxed{\lambda}} c_{\boxed{\lambda}}\Big] \tag{C.29}$$

$$Z_{24}^{\textcircled{\lambda}} = \frac{2\,\mu_{23}^{(\blacksquare)} R_{2\textcircled{\lambda}}}{16\,\left(1-\nu_{\blacksquare}\right)^2}\Big[12\,(\nu_{\blacksquare}-2) q_{\textcircled{\lambda}}^2 a_{\boxed{\lambda}} e_{\boxed{\lambda}} - 12\,q_{\textcircled{\lambda}}^6 e_{\boxed{\lambda}}^2\left(2-3\,\nu_{\blacksquare}\right)$$
$$-24\,q_{\textcircled{\lambda}}^4 d_{\boxed{\lambda}} e_{\boxed{\lambda}} + 16\,\nu_{\blacksquare} a_{\boxed{\lambda}} e_{\boxed{\lambda}} + 8\,\left(2-3\,\nu_{\blacksquare}\right) q_{\textcircled{\lambda}}^6 e_{\boxed{\lambda}} b_{\boxed{\lambda}}$$
$$+24\,q_{\textcircled{\lambda}}^2 e_{\boxed{\lambda}} d_{\boxed{\lambda}}\nu_{\blacksquare} - \frac{4\,\nu_{\blacksquare} a_{\boxed{\lambda}} c_{\boxed{\lambda}}}{q_{\textcircled{\lambda}}^2} + 8\,q_{\textcircled{\lambda}}^4 b_{\boxed{\lambda}} c_{\boxed{\lambda}} - 12\,\nu_{\blacksquare} q_{\textcircled{\lambda}}^2 e_{\boxed{\lambda}} c_{\boxed{\lambda}}\Big] \tag{C.30}$$

$$Z_{34}^{\textcircled{\lambda}} = \frac{4\ \mu_{23}^{(\blacksquare)^2}}{16\ \left(1-\nu_{\blacksquare}\right)^2}\Bigg[18\ q_{\textcircled{\lambda}}^2 a_{\boxed{\lambda}} e_{\boxed{\lambda}} - 18\ q_{\textcircled{\lambda}}^6 e_{\boxed{\lambda}}^2 + 36\ q_{\textcircled{\lambda}}^4 e_{\boxed{\lambda}} d_{\boxed{\lambda}} - 24\ a_{\boxed{\lambda}} e_{\boxed{\lambda}} + 12\ q_{\textcircled{\lambda}}^6 e_{\boxed{\lambda}} b_{\boxed{\lambda}} - 36\ q_{\textcircled{\lambda}}^2 e_{\boxed{\lambda}} d_{\boxed{\lambda}} + \frac{6\ a_{\boxed{\lambda}} c_{\boxed{\lambda}}}{q_{\textcircled{\lambda}}^2} - 12\ q_{\textcircled{\lambda}}^4 b_{\boxed{\lambda}} c_{\boxed{\lambda}} + 18\ q_{\textcircled{\lambda}}^2 e_{\boxed{\lambda}} c_{\boxed{\lambda}}\Bigg] \tag{C.31}$$

and consequently to $\alpha_{\textcircled{\lambda}}^{(i)}$, $A_{\textcircled{\lambda}}$, $B_{\textcircled{\lambda}}$, and $C_{\textcircled{\lambda}}$, which can be factorized by respect to the radius $R_{2\textcircled{\lambda}}$. Let us introduce $\alpha_{\not{R}\textcircled{\lambda}}^{(i)}$, $A_{\not{R}\textcircled{\lambda}}$, $B_{\not{R}\textcircled{\lambda}}$, $C_{\not{R}\textcircled{\lambda}}$ defined as:

$$\left.\begin{aligned} \alpha_{\not{R}\textcircled{\lambda}}^{(i)} &\stackrel{\text{def}}{=} \alpha_{\textcircled{\lambda}}^{(i)} \big/ R_{2\textcircled{\lambda}} \\ A_{\not{R}\textcircled{\lambda}} &\stackrel{\text{def}}{=} A_{\textcircled{\lambda}} \big/ R_{2\textcircled{\lambda}}^2 \\ B_{\not{R}\textcircled{\lambda}} &\stackrel{\text{def}}{=} B_{\textcircled{\lambda}} \big/ R_{2\textcircled{\lambda}}^2 \\ C_{\not{R}\textcircled{\lambda}} &\stackrel{\text{def}}{=} C_{\textcircled{\lambda}} \big/ R_{2\textcircled{\lambda}}^2 \end{aligned}\right\} \tag{C.32}$$

such that μ_{23}^{eff} in Eq. (C.19) writes now:

$$\mu_{23}^{\text{eff}} = \frac{\displaystyle\sum_{i=1}^{2} f_i\ \mu_{23}^{(i)} \sum_{\lambda=1}^{2} \frac{m_\lambda \left(6\ \mu_{23}^{\text{eff}} \alpha_{\not{R}\textcircled{\lambda}}^{(i)} + \beta_{\textcircled{\lambda}}^{(i)}\right)}{A_{\not{R}\textcircled{\lambda}} \mu_{23}^{\text{eff}^2} + B_{\not{R}\textcircled{\lambda}} \mu_{23}^{\text{eff}} + C_{\not{R}\textcircled{\lambda}}}}{\displaystyle\sum_{i=1}^{2} f_i \sum_{\lambda=1}^{2} \frac{m_\lambda \left(6\ \mu_{23}^{\text{eff}} \alpha_{\not{R}\textcircled{\lambda}}^{(i)} + \beta_{\textcircled{\lambda}}^{(i)}\right)}{A_{\not{R}\textcircled{\lambda}} \mu_{23}^{\text{eff}^2} + B_{\not{R}\textcircled{\lambda}} \mu_{23}^{\text{eff}} + C_{\not{R}\textcircled{\lambda}}}} \stackrel{\text{def}}{=} \frac{\underset{\subseteq \mu_{23}^{\text{eff}}}{\{\mathsf{A}_1\}}}{\underset{\subseteq \mu_{23}^{\text{eff}}}{\{\mathsf{A}_2\}}} \tag{C.33}$$

with $\underset{\subseteq \mu_{23}^{\text{eff}}}{\{\mathsf{A}_p\}}$, $p \in [\![1,2]\!]$, given by:

$$\left.\begin{aligned}
\underset{\subseteq \mu_{23}^{\text{eff}}}{\{\mathsf{A}_1\}} &= \frac{m\left[f\mu_{23}^{(1)}\left(6\,\alpha_{\not{R}\textcircled{1}}^{(1)}\mu_{23}^{\text{eff}}+\beta_{\textcircled{1}}^{(1)}\right)+(1-f)\,\mu_{23}^{(2)}\left(6\,\alpha_{\not{R}\textcircled{1}}^{(2)}\mu_{23}^{\text{eff}}+\beta_{\textcircled{1}}^{(2)}\right)\right]}{A_{\not{R}\textcircled{1}}\mu_{23}^{\text{eff}^2}+B_{\not{R}\textcircled{1}}\mu_{23}^{\text{eff}}+C_{\not{R}\textcircled{1}}} \\
&+\frac{(1-m)\left[f\mu_{23}^{(1)}\left(6\,\alpha_{\not{R}\textcircled{2}}^{(1)}\mu_{23}^{\text{eff}}+\beta_{\textcircled{2}}^{(1)}\right)+(1-f)\,\mu_{23}^{(2)}\left(6\,\alpha_{\not{R}\textcircled{2}}^{(2)}\mu_{23}^{\text{eff}}+\beta_{\textcircled{2}}^{(2)}\right)\right]}{A_{\not{R}\textcircled{2}}\mu_{23}^{\text{eff}^2}+B_{\not{R}\textcircled{2}}\mu_{23}^{\text{eff}}+C_{\not{R}\textcircled{2}}} \\
\underset{\subseteq \mu_{23}^{\text{eff}}}{\{\mathsf{A}_2\}} &= \frac{m\left[f\left(6\,\alpha_{\not{R}\textcircled{1}}^{(1)}\mu_{23}^{\text{eff}}+\beta_{\textcircled{1}}^{(1)}\right)+(1-f)\left(6\,\alpha_{\not{R}\textcircled{1}}^{(2)}\mu_{23}^{\text{eff}}+\beta_{\textcircled{1}}^{(2)}\right)\right]}{A_{\not{R}\textcircled{1}}\mu_{23}^{\text{eff}^2}+B_{\not{R}\textcircled{1}}\mu_{23}^{\text{eff}}+C_{\not{R}\textcircled{1}}} \\
&+\frac{(1-m)\left[f\left(6\,\alpha_{\not{R}\textcircled{2}}^{(1)}\mu_{23}^{\text{eff}}+\beta_{\textcircled{2}}^{(1)}\right)+(1-f)\left(6\,\alpha_{\not{R}\textcircled{2}}^{(2)}\mu_{23}^{\text{eff}}+\beta_{\textcircled{2}}^{(2)}\right)\right]}{A_{\not{R}\textcircled{2}}\mu_{23}^{\text{eff}^2}+B_{\not{R}\textcircled{2}}\mu_{23}^{\text{eff}}+C_{\not{R}\textcircled{2}}}
\end{aligned}\right\} \tag{C.34}$$

It is worth noticing that we have used the fact that $A_{\not{R}\textcircled{\lambda}}$, $B_{\not{R}\textcircled{\lambda}}$ and $C_{\not{R}\textcircled{\lambda}}$ only depend on pattern λ but not on phase (i) in Eq. (C.33).

We can now get the final expressions of the eight terms $\alpha_{\not{R}\textcircled{\lambda}}^{(i)}$ and $\beta_{\textcircled{\lambda}}^{(i)}$ (Eq. (B.26)) because $\boldsymbol{Q}^{(0)\textcircled{\lambda}} = \boldsymbol{I}$, an identity array, and because $\boldsymbol{Q}^{(1)\textcircled{\lambda}}$ can be determined by the help of Eq.[95] (69) in Hervé and Zaoui (1995):

$$\left.\begin{aligned}
Q_{14}^{(1)\textcircled{\lambda}} &= 0 \\
Q_{11}^{(1)\textcircled{\lambda}} &= \frac{a_{\boxed{\lambda}}}{4\,\left(1-\nu_{\blacksquare\boldsymbol{\lambda}}\right)q_{\textcircled{\lambda}}^2} \\
Q_{44}^{(1)\textcircled{\lambda}} &= \frac{c_{\boxed{\lambda}}}{4\,\left(1-\nu_{\blacksquare\boldsymbol{\lambda}}\right)} \\
Q_{41}^{(1)\textcircled{\lambda}} &= \frac{-6d_{\boxed{\lambda}}}{4\,\left(1-\nu_{\blacksquare\boldsymbol{\lambda}}\right)}
\end{aligned}\right\} \tag{C.35}$$

leading finally to:

$$\left.\begin{aligned}
\alpha_{\not R\textcircled{\lambda}}^{(\boxed{\lambda})} &= \frac{2}{4\ \left(1-\nu_{\boxed{\lambda}}\right)}\quad \left[\frac{a_{\boxed{\lambda}}}{q_{\textcircled{\lambda}}^2}(3-4\ \nu_{\boxed{\lambda}})+q_{\textcircled{\lambda}}^4(2\ b_{\boxed{\lambda}}-3\ e_{\boxed{\lambda}})\right]\\
\alpha_{\not R\textcircled{\lambda}}^{(\boxed{\lambda})} &= \frac{2}{16\ \left(1-\nu_{\boxed{\lambda}}\right)^2}\left[3\ a_{\boxed{\lambda}}e_{\boxed{\lambda}}\left(1-q_{\textcircled{\lambda}}^2\right)\right.\\
&\qquad \left.+c_{\boxed{\lambda}}q_{\textcircled{\lambda}}^4(2\ b_{\boxed{\lambda}}-3\ e_{\boxed{\lambda}})+\frac{a_{\boxed{\lambda}}c_{\boxed{\lambda}}}{q_{\textcircled{\lambda}}^2}(3-4\ \nu_{\boxed{\lambda}})\right]
\end{aligned}\right\} \tag{C.36}$$

and to:

$$\left.\begin{aligned}
\beta_{\textcircled{\lambda}}^{(\boxed{\lambda})} &= \frac{12\ \mu_{23}^{(\boxed{\lambda})}}{4\ \left(1-\nu_{\boxed{\lambda}}\right)}\quad \left[\frac{a_{\boxed{\lambda}}}{q_{\textcircled{\lambda}}^2}-2\ q_{\textcircled{\lambda}}^4 b_{\boxed{\lambda}}+3\ q_{\textcircled{\lambda}}^4 e_{\boxed{\lambda}}\right]\\
\beta_{\textcircled{\lambda}}^{(\boxed{\lambda})} &= \frac{12\ \mu_{23}^{(\boxed{\lambda})}}{16\ \left(1-\nu_{\boxed{\lambda}}\right)^2}\left[-2\ c_{\boxed{\lambda}}b_{\boxed{\lambda}}q_{\textcircled{\lambda}}^4+3\ a_{\boxed{\lambda}}e_{\boxed{\lambda}}q_{\textcircled{\lambda}}^4\right.\\
&\qquad \left.+3\ a_{\boxed{\lambda}}e_{\boxed{\lambda}}(q_{\textcircled{\lambda}}^2-1)+6\ e_{\boxed{\lambda}}d_{\boxed{\lambda}}q_{\textcircled{\lambda}}^4+\frac{a_{\boxed{\lambda}}c_{\boxed{\lambda}}}{q_{\textcircled{\lambda}}^2}\right]
\end{aligned}\right\} \tag{C.37}$$

We can also get the final expressions of $A_{\not R\textcircled{\lambda}}$, $B_{\not R\textcircled{\lambda}}$, $C_{\not R\textcircled{\lambda}}$.

$A_{\not R\textcircled{\lambda}}$ is given by:

$$A_{\not R\textcircled{\lambda}} \stackrel{\text{def}}{=} \underset{\subseteq A_{\not R\textcircled{\lambda}}}{\{\mathsf{A}_1\}} + \frac{\underset{\subseteq A_{\not R\textcircled{\lambda}}}{\{\mathsf{A}_2\}}}{k_{23}^{\text{eff}}} \tag{C.38}$$

where

$$\begin{aligned}
\underset{\subseteq A_{\not R\textcircled{\lambda}}}{\{\mathsf{A}_1\}} &= \frac{12\ Z_{12}^{\textcircled{\lambda}}}{R_{2\textcircled{\lambda}}^2}\\
&= \frac{12}{4\ \left(1-\nu_{\boxed{\lambda}}\right)^2}\left[-6\ q_{\textcircled{\lambda}}^2 a_{\boxed{\lambda}}e_{\boxed{\lambda}}-6\ q_{\textcircled{\lambda}}^2 e_{\boxed{\lambda}}c_{\boxed{\lambda}}+12\ q_{\textcircled{\lambda}}^2 d_{\boxed{\lambda}}e_{\boxed{\lambda}}\right.\\
&+4\ q_{\textcircled{\lambda}}^6 b_{\boxed{\lambda}}e_{\boxed{\lambda}}\left(3-4\ \nu_{\boxed{\lambda}}\right)+6\ q_{\textcircled{\lambda}}^6 e_{\boxed{\lambda}}^2\left(4\ \nu_{\boxed{\lambda}}-3\right)+4\ q_{\textcircled{\lambda}}^4 b_{\boxed{\lambda}}c_{\boxed{\lambda}}\\
&\left.-12\ q_{\textcircled{\lambda}}^4 e_{\boxed{\lambda}}d_{\boxed{\lambda}}+\frac{2\ a_{\boxed{\lambda}}c_{\boxed{\lambda}}}{q_{\textcircled{\lambda}}^2}\left(3-4\ \nu_{\boxed{\lambda}}\right)+8\ a_{\boxed{\lambda}}e_{\boxed{\lambda}}\left(3-6\ \nu_{\boxed{\lambda}}+4\ \nu_{\boxed{\lambda}}^2\right)\right]
\end{aligned} \tag{C.39}$$

and

$$\begin{aligned}\underset{\subseteq A_{\not R\textcircled{\lambda}}}{\{\mathsf{A}_2\}} &= \frac{6}{R_{2\textcircled{\lambda}}}\left(Z_{14}^{\textcircled{\lambda}}+Z_{32}^{\textcircled{\lambda}}+Z_{24}^{\textcircled{\lambda}}+Z_{31}^{\textcircled{\lambda}}\right)\\ &= \frac{12\ \mu_{23}^{(\blacksquare)}}{16\ \left(1-\nu_{\blacksquare}\right)^2}\Bigg[-12\ q_{\textcircled{\lambda}}^2 a_{\boxed{\lambda}}e_{\boxed{\lambda}}+12\ q_{\textcircled{\lambda}}^6 e_{\boxed{\lambda}}^2-24\ q_{\textcircled{\lambda}}^4 d_{\boxed{\lambda}}e_{\boxed{\lambda}}\\ &\qquad +16\ \nu_{\blacksquare}a_{\boxed{\lambda}}e_{\boxed{\lambda}}-8\ q_{\textcircled{\lambda}}^6 b_{\boxed{\lambda}}e_{\boxed{\lambda}}+24\ q_{\textcircled{\lambda}}^2 d_{\boxed{\lambda}}e_{\boxed{\lambda}}\\ &\qquad +\frac{4\ a_{\boxed{\lambda}}c_{\boxed{\lambda}}}{q_{\textcircled{\lambda}}^2}\left(3-4\ \nu_{\blacksquare}\right)+8\ q_{\textcircled{\lambda}}^4 b_{\boxed{\lambda}}c_{\boxed{\lambda}}-12\ q_{\textcircled{\lambda}}^2 e_{\boxed{\lambda}}c_{\boxed{\lambda}}\Bigg]\end{aligned} \tag{C.40}$$

$B_{\not R\textcircled{\lambda}}$ is given by:

$$B_{\not R\textcircled{\lambda}} \overset{\text{def}}{=} \underset{\subseteq B_{\not R\textcircled{\lambda}}}{\{\mathsf{A}_1\}}+\frac{\underset{\subseteq B_{\not R\textcircled{\lambda}}}{\{\mathsf{A}_2\}}}{k_{23}^{\text{eff}}} \tag{C.41}$$

where

$$\begin{aligned}\underset{\subseteq B_{\not R\textcircled{\lambda}}}{\{\mathsf{A}_1\}} &= \frac{2}{R_{2\textcircled{\lambda}}}\left(2Z_{14}^{\textcircled{\lambda}}+2Z_{32}^{\textcircled{\lambda}}+Z_{24}^{\textcircled{\lambda}}+Z_{31}^{\textcircled{\lambda}}\right)\\ &= \frac{8\ \mu_{23}^{(\blacksquare)}}{16\ \left(1-\nu_{\blacksquare}\right)^2}\Bigg[36\ \left(1-\nu_{\blacksquare}\right)q_{\textcircled{\lambda}}^6 e_{\boxed{\lambda}}^2\\ &\qquad +24\ \left(\nu_{\blacksquare}-1\right)q_{\textcircled{\lambda}}^6 e_{\boxed{\lambda}}b_{\boxed{\lambda}}+12\ \left(1-\nu_{\blacksquare}\right)\frac{a_{\boxed{\lambda}}c_{\boxed{\lambda}}}{q_{\textcircled{\lambda}}^2}\Bigg]\end{aligned} \tag{C.42}$$

and

$$\begin{aligned}\underset{\subseteq B_{\not R\textcircled{\lambda}}}{\{\mathsf{A}_2\}} &= 2\ Z_{34}^{\textcircled{\lambda}}\\ &= \frac{8\ \mu_{23}^{(\blacksquare)^2}}{16\ \left(1-\nu_{\blacksquare}\right)^2}\Bigg[18\ q_{\textcircled{\lambda}}^2 a_{\boxed{\lambda}}e_{\boxed{\lambda}}-18\ q_{\textcircled{\lambda}}^6 e_{\boxed{\lambda}}^2+36\ q_{\textcircled{\lambda}}^4 e_{\boxed{\lambda}}d_{\boxed{\lambda}}\\ &\qquad -24\ a_{\boxed{\lambda}}e_{\boxed{\lambda}}+12\ q_{\textcircled{\lambda}}^6 e_{\boxed{\lambda}}b_{\boxed{\lambda}}-36\ q_{\textcircled{\lambda}}^2 e_{\boxed{\lambda}}d_{\boxed{\lambda}}\\ &\qquad +\frac{6\ a_{\boxed{\lambda}}c_{\boxed{\lambda}}}{q_{\textcircled{\lambda}}^2}-12\ q_{\textcircled{\lambda}}^4 b_{\boxed{\lambda}}c_{\boxed{\lambda}}+18\ q_{\textcircled{\lambda}}^2 e_{\boxed{\lambda}}c_{\boxed{\lambda}}\Bigg]\end{aligned} \tag{C.43}$$

776 $C_{\not{R}\textcircled{\lambda}}$ is given by:

$$\begin{aligned} C_{\not{R}\textcircled{\lambda}} &= Z_{34}^{\textcircled{\lambda}} \\ &= \frac{4\ \mu_{23}^{(\blacksquare)^2}}{16\ \left(1-\nu_{\blacksquare}\right)^2}\Bigg[18\ q_{\textcircled{\lambda}}^2 a_{\boxed{\lambda}} e_{\boxed{\lambda}} - 18\ q_{\textcircled{\lambda}}^6 e_{\boxed{\lambda}}^2 + 36\ q_{\textcircled{\lambda}}^4 e_{\boxed{\lambda}} d_{\boxed{\lambda}} \\ &\qquad -24\ a_{\boxed{\lambda}} e_{\boxed{\lambda}} + 12\ q_{\textcircled{\lambda}}^6 e_{\boxed{\lambda}} b_{\boxed{\lambda}} - 36\ q_{\textcircled{\lambda}}^2 e_{\boxed{\lambda}} d_{\boxed{\lambda}} \\ &\qquad +\frac{6\ a_{\boxed{\lambda}} c_{\boxed{\lambda}}}{q_{\textcircled{\lambda}}^2} - 12\ q_{\textcircled{\lambda}}^4 b_{\boxed{\lambda}} c_{\boxed{\lambda}} + 18\ q_{\textcircled{\lambda}}^2 e_{\boxed{\lambda}} c_{\boxed{\lambda}}\Bigg] \end{aligned} \tag{C.44}$$

References

Albérola, N., Bas, C., and Mélé, P. (1994). Composites particulaires : modelisation du comportement viscoelastique, assortie du concept de percolation. *C. R. Acad. Sci. Paris, Série II*, 319:1129–1134.

Bardella, L. and Genna, F. (2001). On the elastic behavior of syntactic foams. *Int. J. Sol. Structures*, 38:7235–7260.

Bardella, L., Perini, G., Panteghini, A., Tessier, N., Gupta, N., and Porfiri, M. (2018). Failure of glass-microballoons/thermoset-matrix syntactic foams subject to hydrostatic loading. *European Journal of Mechanics - A/Solids*, 70:58 – 74.

Bilger, N., Auslender, F., Bornert, M., Moulinec, H., and Zaoui, A. (2007). Bounds and estimates for the effective yield surface of porous media with a uniform or a nonuniform distribution of voids. *Eur. J. Mech., A/Solids*, 26:810–836.

Bornert, M., Stolz, C., and Zaoui, A. (1996). Morphologically representative pattern-based bounding in elasticity. *J. Mech. Phys. Sol.*, 44:307–331.

Christensen, R. M. and Lo, K. H. (1979). Solutions for the effective shear properties in three phase sphere and cylinder models. *J. Mech. Phys. Sol.*, 27:315–330.

Diani, J. and Gilormini, P. (2014). Using a pattern-based homogenization scheme for modeling the linear viscoelasticity of nano-reinforced polymers with an interphase. *J. Mech. Phys. Sol.*, 63:51–61.

Gusev, A., Hine, P., and Ward, I. (2000). Fiber packing and elastic properties of transversely random unidirectional glass/epoxy composite. *Composite Science Technology*, 60:535–541.

Hashin, Z. and Rosen, B. W. (1964). The elastic moduli of fiber-reinforced materials. *J. of Applied Mechanics*, 31:223–230.

Hervé, E., Stolz, C., and Zaoui, A. (1991). A propos de l'assemblage de sphères composites de hashin. *C. R. Acad. Sci. Paris, Série II*, 313:857–852.

Hervé, E. and Zaoui, A. (1995). Elastic behaviour of multiply coated fibrer-reinforced composites. *Int. J. of Engng Science*, 33:1419–1433.

Hervé-Luanco, E. (2020). Elastic behaviour of multiply coated fibre-reinforced composites: Simplification of the (n+1)-phase model and extension to imperfect interfaces. *International Journal of Solids and Structures*, 196-197:10 – 25.

Hervé-Luanco, E. and Joannès, S. (2016). Multiscale modelling of transport phenomena for materials with n-layered embedded fibres. part i: Analytical and numerical-based approaches. *Int. J. Sol. Structures*, 97-98:625–636.

Hill, R. (1963). Elastic properties of reinforced solids: Some theoretical principles. *Journal of the Mechanics and Physics of Solids*, 11(5):357 – 372.

Joannès, S. and Hervé-Luanco, E. . (2016). Multiscale modelling of transport phenomena for materials with n-layered embedded fibres. part ii: Investigation of fibre packing effects. *Int. J. Sol. Structures*, 97-98:566–574.

Majewski, M., Kursa, M., and Kowalczyk-Gajewska, K. (2017). Micromechanical and numerical analysis of packing and size effects in elastic particulate composites. *Composites Part B*, 124:158–174.

Marcadon, V., Herve, E., and Zaoui, A. (2007). Micromechanical modeling of packing and size effects in particulate composites. *Int. J. Sol. Structures*, 44:8213–8228.

Markham, M. F. (1970). Measurement of the elastic constants of fibre composites by ultrasonics. *COMPOSITE*, pages 145–149.

Mélé, P., Marceau, S., Brown, D., and Albérola, N. (2005). Conséquences de l'agrégation et de la percolation de charges sur le comportement viscoélastique de nanocomposites. *C. R. Mecanique*, 333:155–161.

Paterson, D. A. P., Ijomah, W., and Windmill, J. (2018). Elastic constant determination of unidirectional composite via ultrasonic bulk wave through transmission measurements: A review. *Progress in Materials Science*, 97:1–37.

Zimmer, J. and Cost, J. (1970). Determination of the elastic constants of an unidirectional fiber composite using ultrasonic velocity measurements. *J. Acoust. Soc. Am*, 47:795–803.